

Characterization of the genetic switch from phage phi13 important for *Staphylococcus aureus* colonization in humans

Journal:	<i>MicrobiologyOpen</i>
Manuscript ID	MBO32021070375.R1
Wiley - Manuscript type:	Original Article
Date Submitted by the Author:	19-Sep-2021
Complete List of Authors:	Kristensen, Camilla; Technical University of Denmark, Department of Biotechnology and Biomedicine Varming, Anders; University of Copenhagen, Department of Chemistry Leinweber, Helena; University of Copenhagen Faculty of Life sciences, Department of Veterinary and Animal Sciences Hammer, Karin; Technical University of Denmark Lo Leggio, Leila; University of Copenhagen, Department of Chemistry Ingmer, Hanne; University of Copenhagen Faculty of Life sciences, department of Veterinary and Animal Sciences Kilstrup, Mogens ; Technical University of Denmark, Department of Biotechnology and Biomedicine
Search Terms:	bacteriophages, phenotypic switch, <i>Staphylococcus</i>
Abstract:	Temperate phages are bacterial viruses that either reside integrated into a bacterial genome as lysogens or enter a lytic lifecycle. The decision between lifestyles is determined by a switch involving a phage-encoded repressor, <i>CI</i> , and a promoter region from which lytic and lysogenic genes are divergently transcribed. Here we investigate the switch of phage phi13 from the human pathogen <i>Staphylococcus aureus</i> . phi13 encodes several virulence factors and is prevalent in <i>S. aureus</i> strains colonizing humans. We show that the phi13 switch harbors a <i>cI</i> gene, a predicted <i>mor</i> (modulator of repression) gene, and three high-affinity operator sites binding <i>CI</i> . To quantify the decision between lytic and lysogenic lifestyle, we introduced reporter plasmids that carry the 1.3 kb switch region from phi13 with the lytic promoter fused to <i>lacZ</i> into <i>S. aureus</i> and <i>B. subtilis</i> . Analysis of beta-galactosidase expression indicated that decision frequency is independent of host factors. The white "lysogenic" phenotype, which relies on expression of <i>cI</i> , could be switched to a stable blue "lytic" phenotype by DNA damaging agents. We have characterized lifestyle decisions of phage phi13, and our approach may be applied to other temperate phages encoding virulence factors in <i>S. aureus</i> .

1
2
3
4
5
6
7
8
9
10
11
12
13
14
15
16
17
18
19
20
21
22
23
24
25
26
27
28
29
30
31
32
33
34
35
36
37
38
39
40
41
42
43
44
45
46
47
48
49
50
51
52
53
54
55
56
57
58
59
60



1
2
3
4 **Characterization of the genetic switch from phage ϕ 13 important for *Staphylococcus aureus***
5 **colonization in humans**
6
7

8
9
10 Camilla S. Kristensen (Camilla_S_K@hotmail.com)^a, Anders K. Varming
11 (anders.varming@chem.ku.dk)^b, Helena A. K. Leinweber (helena.leinweber@sund.ku.dk)^c, Karin
12 Hammer (kha@bio.dtu.dk)^a, Leila Lo Leggio (leila@chem.ku.dk)^b, Hanne Ingmer (hi@sund.ku.dk)^c,
13 **Mogens Kilstrup (mki@bio.dtu.dk, tlf. +45 2113 8815)^a**
14
15

16
17 ^a Department of Biotechnology and Biomedicine, Technical University of Denmark, Denmark

18
19 ^b Department of Chemistry, University of Copenhagen, Denmark

20
21 ^c Department of Veterinary and Animal Sciences, University of Copenhagen, Denmark
22
23

24 **ORCID ID**

25
26 Camilla S. Kristensen: 0000-0001-6564-8455

27
28 Anders K. Varming: 0000-0001-6865-990X

29
30 Helena A. K. Leinweber: 0000-0002-9949-819X

31
32 Karin Hammer: 0000-0002-6250-8067

33
34 Leila Lo Leggio: 0000-0002-5135-0882

35
36 Hanne Ingmer: 0000-0002-8350-5631

37
38 Mogens Kilstrup: 0000-0002-3900-723X
39
40
41
42
43
44
45
46
47
48
49
50
51
52
53
54
55
56
57
58
59
60

ABSTRACT

Temperate phages are bacterial viruses that after infection either reside integrated into a bacterial genome as prophages forming lysogens or multiply in a lytic lifecycle. The decision between lifestyles is determined by a switch involving a phage-encoded repressor, *CI*, and a promoter region from which lytic and lysogenic genes are divergently transcribed. Here we investigate the switch of phage $\phi 13$ from the human pathogen *Staphylococcus aureus*. $\phi 13$ encodes several virulence factors and is prevalent in *S. aureus* strains colonizing humans. We show that the $\phi 13$ switch harbors a *cl* gene, a predicted *mor* (modulator of repression) gene, and three high-affinity operator sites binding *CI*. To quantify the decision between lytic and lysogenic lifestyle, we introduced reporter plasmids that carry the 1.3 kb switch region from $\phi 13$ with the lytic promoter fused to *lacZ* into *S. aureus* and *B. subtilis*. Analysis of β -galactosidase expression indicated that decision frequency is independent of host factors. The white "lysogenic" phenotype, which relies on the expression of *cl*, could be switched to a stable blue "lytic" phenotype by DNA damaging agents. We have characterized lifestyle decisions of phage $\phi 13$, and our approach may be applied to other temperate phages encoding virulence factors in *S. aureus*.

KEYWORDS

bacteriophage, prophage, lysogeny, genetic switch, *Staphylococcus aureus*, repressor, $\phi 13$, phi13

INTRODUCTION

Staphylococcus aureus is a Gram-positive, opportunistic human pathogen causing millions of infections worldwide each year, ranging from skin and soft tissue infections, food poisoning, endocarditis, and respiratory tract infections to bacteremia, amongst many others (Lowy, 1998; Liu, 2009; Tong *et al.*, 2015). The severity of the infections varies from mild to life-threatening, largely determined by the various virulence factors contained in the infecting strain.

A number of important virulence factors are encoded by *S. aureus* prophages that stably reside in the bacterial genome (Xia and Wolz, 2014). Most clinical strains of *S. aureus* are lysogens and carry between one and four prophages that encode important toxins, such as Panton-Valentine leucocidin (PVL) and enterotoxins (Ingmer, Gerlach and Wolz, 2019). Some of the most common prophages in

1
2
3
4 human isolates of *S. aureus* belong to the Sa3int group. These phages integrate into the *hly* gene of
5
6 *S. aureus* and express an immune evasion cluster encoding several virulence factors promoting
7
8 colonization (Coleman *et al.*, 1991; Xia and Wolz, 2014). As the beta-hemolysin encoded by *hly* is
9
10 also a virulence factor (Huseby *et al.*, 2007; Katayama *et al.*, 2013), this negative conversion appears
11
12 counterintuitive, but Sa3int phages have been shown to excise and remain as pseudo-lysogens,
13
14 allowing expression of both the beta-hemolysin and the virulence factors encoded by the phage
15
16 (Goerke *et al.*, 2006; Katayama *et al.*, 2013; Salgado-Pabón *et al.*, 2014).
17

18
19 Temperate phages have a dual lifecycle involving either lytic replication and production of active
20
21 phages or being inserted in and replicated with the bacterial chromosome. The decision between
22
23 these lifestyles is made by a phage-encoded (epi)genetic switch. Phage λ , targeting *Escherichia coli*,
24
25 offers the classical example of such a switch, where a complex decision phase determines from
26
27 which of the two involved promoters, P_R or P_{RM} , transcription occurs. Expression from the P_{RM}
28
29 promoter produces the phage repressor CI, whereas expression from P_R allows the production of
30
31 the Cro repressor, as well as other gene products needed for producing active phage particles
32
33 (Oppenheim *et al.*, 2005; Casjens and Hendrix, 2015). Stable expression from the P_{RM} promoter is
34
35 needed for the maintenance of the λ chromosome into the *E. coli* chromosome. It also produces a
36
37 high concentration of the CI repressor, which is required for activation of the P_{RM} promoter and tight
38
39 repression of the P_R promoter in the integrated prophage and any incoming λ phages, rendering the
40
41 lysogenic bacterium immune to secondary attacks. The decision and integration of phage λ are not
42
43 solely dependent upon the phage-encoded factors, as *E. coli* host factors also affect this process
44
45 (Grodzicker, Arditti and Eisen, 1972; Herman *et al.*, 1993; Kihara, Akiyama and Ito, 2001; Roucourt
46
47 and Lavigne, 2009). The escape of phage λ from the lysogenic state can be initiated by autocleavage
48
49 of the CI repressor. In a process analogous to autocleavage of the LexA repressor, CI is bound to
50
51 activated RecA filaments polymerized on single-stranded DNA during the SOS DNA damage
52
53 response, leading to activation of CI auto-peptidase activity (Little, 1984; Oppenheim *et al.*, 2005;
54
55 Atsumi and Little, 2006). A quite different switch mechanism is used by the TP901-1 phage infecting
56
57 the Gram-positive bacterium *Lactococcus lactis* (Madsen *et al.*, 1999) which shares extensive
58
59 homology to the ϕ 13 switch (Pedersen *et al.*, 2020). Here, a CI repressor, expressed from the
60
lysogenic promoter P_R , represses the lytic P_L promoter. A small repressor (MOR, for modulator of

1
2
3
4 repression) expressed from the P_L promoter represses the P_R promoter; however, it does require CI
5 as a co-repressor. In addition MOR functions as an anti-repressor against CI (Pedersen and Hammer,
6 2008).
7
8
9

10
11 As a member of the staphylococcal Sa3int phage family, the bacteriophage $\phi 13$ shares features with
12 the other members. These features include the Sa3 type integrase and the presence of the *sak*, *chp*,
13 and *scn* virulence genes (Goerke *et al.*, 2009; Xia and Wolz, 2014), but an analysis of the genetic
14 switches within the group has never been reported.
15
16
17
18
19

20
21 To characterize the switch from phage $\phi 13$, we have compared its switch region to the switch
22 regions in TP901-1 and the switch regions in *Staphylococcus* phages, showing that a group of phages
23 with the Sa3 integrase shares similar switch regions containing CI and MOR homologs. We have
24 purified the $\phi 13$ CI repressor and shown that it interacts with three palindromic sites in the switch
25 region. By constructing plasmids containing the $\phi 13$ genetic switch with *lacZ* reporter fusions to the
26 lytic promoter (switch plasmids) and analysis of the frequency of Lac phenotypes in transformants
27 of the natural and a heterologous host, we have shown that a functional *mor* gene is required for
28 “decision switching” and that this process is independent of staphylococcal host factors. The
29 concept of “toggle switching” has previously been defined as “the induced or accidental change
30 from one stable phenotype to another from a bistable switch” (Gardner, Cantor, and Collins, 2000).
31 Thus, toggle switching is when the phage changes its state, either spontaneously or following
32 induction. In contrast, decision switching is when the phage initially establishes itself as lytic or
33 lysogenic, in a process that precedes toggle switching. In the current study, $\phi 13$ switch plasmids
34 were found to toggle spontaneously from the “lytic” (Lac+, blue) colony phenotype to a stable
35 “lysogenic” (Lac-, white) colony phenotype. In the opposite direction, toggling from the stable
36 “lysogenic” colony phenotype to the “lytic” colony phenotype could readily be induced by sub-lethal
37 concentrations of DNA damaging agents. The results from this study can prove important in the
38 analysis of *S. aureus* virulence *in vivo* by determining conditions during infection that would result
39 in induction and spread of $\phi 13$ and the unwanted establishment of $\phi 13$ prophages in susceptible
40 hosts. The results may ultimately aid in the understanding of how some Sa3int prophages are
41 disseminated in society and suggest ways to limit *S. aureus* colonization in humans.
42
43
44
45
46
47
48
49
50
51
52
53
54
55
56
57
58
59
60

EXPERIMENTAL PROCEDURES

Growth specifications

Unless otherwise specified, *E. coli* and *B. subtilis* were grown in lysogeny broth (LB) or LB agar, while *S. aureus* was grown in tryptic soy broth (TSB) or agar (TSA). All strains were grown at 37 °C with sufficient aeration and the addition of appropriate antibiotics. 5-bromo-4-chloro-3-indolyl- β -D-galactopyranoside (X-gal) was added to agar plates at 100-200 $\mu\text{g ml}^{-1}$.

Phages were stored and diluted in SM buffer (100 mM NaCl, 8 mM $\text{MgSO}_4 \cdot 7\text{H}_2\text{O}$, 50 mM Tris-CL (pH 7.5)).

Bacterial strains and plasmids

All bacterial strains used in this study can be found in Appendix Table 1, while selected strains, plasmids, and phages are summarized in Table 1, 2, and 3, respectively.

Protein expression and purification

A synthetic codon-optimized gene for recombinant CI repressor protein with an N-terminal His-tag and TEV cleavage site (ϕ 13 rCI) was purchased from Genscript (Appendix Fig. 1) in a pET30a(+) expression vector. The expression vector was transformed into BL21 (DE3) *E. coli* cells and grown at 37 °C. ϕ 13 rCI expression was induced by 0.5 mM isopropyl β -D-1-thiogalactopyranoside in a mid-exponential culture and the temperature lowered to 25 °C.

After 20 hours, cells were harvested and sonicated. The cell lysate was collected and filtered through a 0.22 μm filter. Chromatographic purification was done on an ÄKTA purifier 10 system (GE Healthcare Life Sciences) by immobilized metal affinity chromatography (IMAC) (HisTrap HP 1 ml column) and size exclusion chromatography (SEC) (HiLoad 26/600 Superdex200 column). 20 mM Tris, 20 mM imidazole, 1 M NaCl, pH 8.0 was used as washing buffer and 20 mM Tris, 500 mM imidazole, 100 mM NaCl, pH 8.0 as elution buffer in IMAC, while 20 mM Tris, 100 mM NaCl, pH 7.5 was used as SEC buffer. Blue Dextran (2000 kDa), Ferritin (440 kDa), Catalase (232 kDa), Aldolase (158 kDa), Carbonic Anhydrase (29 kDa), and Aprotinin (6.5 kDa) were used as Mw standards in SEC. Protein purity was assessed by SDS-PAGE (15 % gels).

1
2
3
4
5
6
7
8
9
10
11
12
13
14
15
16
17
18
19
20
21
22
23
24
25
26
27
28
29
30
31
32
33
34
35
36
37
38
39
40
41
42
43
44
45
46
47
48
49
50
51
52
53
54
55
56
57
58
59
60

The protein concentration was estimated by A_{280} using an extinction coefficient of $26360 \text{ M}^{-1} \text{ cm}^{-1}$ (tagged) and $23380 \text{ M}^{-1} \text{ cm}^{-1}$ (untagged) as estimated with ProtParam (<http://web.expasy.org/protparam>) (Gasteiger *et al.*, 2005).

For EMSA using native CI, the tag on $\phi 13$ rCI was removed beforehand by mixing the protein 10:1 with TEV protease (Sigma Aldrich) and incubating it at $4 \text{ }^\circ\text{C}$ for 3 days. The uncleaved protein was separated from the mixture by IMAC and the flowthrough was collected for use.

DSF and CD spectroscopy

The inflection temperature, T_i , was determined using a Nanotemper Tycho™ NT.6 DSF monitoring changes in the ratio of intrinsic fluorescence at 350 and 330 nm while heating from 35 to $95 \text{ }^\circ\text{C}$ with a temperature ramp of $30 \text{ }^\circ\text{C min}^{-1}$. The sample was loaded in high precision glass capillaries with a concentration of $4.9 \text{ }\mu\text{M}$.

For CD spectroscopy, the purified protein was transferred to a 20 mM NaF buffer, pH 7.5. The experiments were conducted on a Jasco J-815 CD spectropolarimeter in a suprasil quartz cell with a 1 mm light path (Hellma Analytics) and a sample concentration of $1.56 \text{ }\mu\text{M}$. The spectra were measured at room temperature in a continuous mode at 20 nm min^{-1} from 260 to 190 nm with a data pitch and bandwidth of 1 nm , averaging five spectra per measurement and subtracting the buffer spectra. The CD spectrum was deconvoluted and analyzed using DichroWeb (Whitmore and Wallace, 2008) with the CDSSTR method (Sreerama and Woody, 2000) and reference sets 3 and 6 and by BeStSel (Micsonai *et al.*, 2015, 2018).

Synthesis and labeling of DNA fragments

For gel shift assays, DNA fragments containing each of the three operator sites, O_R , O_L and O_D , were synthesized by PCR with appropriate annealing temperatures using a Phusion polymerase. Non-fluorescent probes were created by amplifying the genetic switch region of $\phi 13$ with primers MK867 and MK868 for O_R , MK869 and MK870 for O_L , and MK871 and MK872 for O_D . The DNA fragments were made fluorescent by a second PCR run with the Cy5-containing primers MK740 and MK741. Mutated probes with altered operator half-sites (TTCA to TTGA) were amplified from the non-

1
2
3
4 fluorescent probes in two steps. First overlapping left and right half parts were amplified: O_R left
5 part from the O_R probe using MK1038 and MK741; O_R right part from the O_R probe using MK1039
6 and MK740; O_L left part from the O_L probe using MK1040 and MK741; O_L right part from the O_L
7 probe using MK1041 and MK740; O_D left part from the O_D probe using MK1042 and MK741; O_D right
8 part from the O_D probe using MK1043 and MK740. Full-length mutant probes were synthesized with
9 the overlapping left parts and right parts as templates and mega-primers in a subsequent PCR
10 reaction, followed by amplification of the product with fluorescent primers MK740 and MK741. See
11 Appendix Table 2 for a list of primers used in this study.
12
13
14
15
16
17
18
19
20

21 **EMSA**

22 Tagged and detagged ϕ 13 rCI was mixed with binding buffer (100 mM Tris-HCl, 5 mM EDTA, 500
23 mM NaCl, 5 mM DTT, 25 % glycerol), bovine serum albumin, and sheared DNA. In each assay,
24 approximately 0.5 nM DNA probe was mixed with varying concentrations of rCI in a total of 20 μ l
25 binding solution. After pre-incubation on ice for 15 min, the DNA fragment was added and
26 incubation was continued for 30 min. The mixture was then transferred into the empty wells of a
27 chilled 2 % agarose gel and run horizontally in 1x TBE (Tris/Borate/EDTA) buffer for 90 min at a
28 constant voltage of 110 at 0°C. For visualization and quantification, the gel was scanned directly in
29 a STORM 860 Imager (Amersham Biosciences) using the red channel (635 nm) at high sensitivity,
30 followed by image editing using the ImageQuant TL software (Amersham Biosciences). The image
31 was analyzed using Fiji (Schindelin *et al.*, 2012). The integrated density of each band was measured
32 and used to calculate the individual fractions of protein bound to DNA at each protein
33 concentration. The data were fitted with the following binding equation using Microsoft Excel
34 (version 16.48 with Solver add-in) to perform non-linear regression and obtain a value for K_D:
35 Fraction bound = $B_{\max}([protein]/(K_D + [protein]))$, where B_{max} is the fraction bound at which the data
36 plateau.
37
38
39
40
41
42
43
44
45
46
47
48
49
50
51

52 **Construction of switch plasmids**

53 All PCRs were conducted at appropriate annealing temperature and elongation time using Phusion
54 polymerase unless otherwise specified. All switch plasmids contained the entire genetic switch of
55 ϕ 13 with a *lacZ* gene translationally fused to P_L downstream of *mor*, and all constructs were verified
56
57
58
59
60

1
2
3
4 by sequencing. pCSK2 was created by amplifying the genetic switch region of ϕ 13 from 8325-4 ϕ 13
5 with primers MK860 and MK863, digestion by EcoRI and BamHI, followed by ligation into digested
6 pDG1729. From pCSK2, the switch region and *lacZ* gene were amplified by primers MK863 and
7 MK902, digested by EcoRI and BglII, and ligated into pCL25 digested by EcoRI and BamHI creating
8 pCSK9. pCSK3 was constructed by amplifying the switch region of ϕ 13 from 8325-4 ϕ 13 with primers
9 MK861 and MK862, digestion by XbaI and SphI, followed by ligation into digested pNZlac. The start
10 codon of *mor* was mutated (ATG to ATC) in pCSK2, pCSK3, and pCSK9 by use of CloneAmp™ HiFi PCR
11 Premix Polymerase resulting in pCSK11, pCSK13, and pCSK12. The primers MK914 and MK915 were
12 used to amplify the entire plasmid while incorporating the point mutation.
13
14
15
16
17
18
19
20
21
22

23 **Transformations**

24 Electrocompetent *E. coli* cells were created and electroporated as previously described (Pedersen
25 *et al.*, 2020). Cells were plated on selective agar plates after 1 h of recovery.
26
27

28 Competent *B. subtilis* cells were obtained as described in (Konkol, Blair, and Kearns, 2013) with one
29 minor change; 30 min after plasmid addition equal volumes of LB media were added to the
30 transformation mixture, followed by incubation for 1 h and plating on selective plates.
31
32

33 Transformations in *S. aureus* were performed using the procedure for electroporation described in
34 (Monk *et al.*, 2015). pYL112 Δ 19 was transformed into 8325-4 and 8325-4 ϕ 13-kana before the
35 introduction of integrating plasmids to supply the required integrase.
36
37
38
39
40

41 **Transductions**

42 Transductions in *B. subtilis* and *S. aureus* were accomplished by using phage SPP1 or ϕ 11/ ϕ 80 α ,
43 respectively. See Table 3 for all phages used in this study. Transducing phage stocks were prepared
44 as plate lysates on the donor strains by allowing phage adsorption for 15 min at 37 °C with 5 mM
45 CaCl₂ and subsequent plating in top agar (LB/TSB, 0.5 % agar, 5 mM CaCl₂). After overnight
46 incubation, the top layer was suspended in SM, centrifuged at 5.000 g for 10 min, and the
47 supernatant was filter-sterilized (0.2 μ m). Transducing phages were added at a multiplicity of
48 infection (MOI) of 10 to *B. subtilis* 168 and MOI = 0.1 to *S. aureus* 8325-4 and 8325-4 ϕ 13, followed
49 by 15 min incubation at 37 °C. Cells were washed with equal volumes of 20 mM Na-citrate and
50 plated on selective plates containing X-gal and 20 mM Na-Citrate.
51
52
53
54
55
56
57
58
59
60

Stability of switch plasmid phenotypes

To examine the stability of the “lysogenic” and “lytic” phenotype of the switch plasmids, a single colony resulting from transformation was suspended in an appropriate medium, diluted, and plated at a density allowing the formation of single colonies for phenotype determination.

Plate inductions

To test the effect of inducing substances, both *B. subtilis* and *S. aureus* cells containing switch plasmids were plated at a cell density resulting in around 1000 colonies per plate, obtained by suspending a colony in LB/TSA medium, dilutions, and plating. 3 μl inducing substance (0.5 mg ml^{-1} mitomycin C, 1 mg ml^{-1} ciprofloxacin, or 30 % hydrogen peroxide) was applied to the middle of the plate, followed by incubation at 37 °C. When relevant, selected colonies were suspended in media, diluted, and plated at a density resulting in single colonies to determine phenotypes.

Temporal induction

A culture of 8325-4 *geh::pCSK9* favoring the “lysogenic” phenotype (CSK48) was inoculated in TSB and grown to $\text{OD}_{600}=0.6$ followed by induction by 1 $\mu\text{g ml}^{-1}$ mitomycin C. Samples were taken periodically, diluted in TSB, and plated on selective TSA plates containing X-gal. Switch plasmid phenotypes were determined after overnight incubation.

Phage infection of 8325-4 harboring switch plasmids

Cultures were inoculated in TSB and grown to $\text{OD}_{600}=0.6$. At this point a sample was plated for determination of colony forming units (CFU) ml^{-1} , after which, phages were added at a MOI of 0.1, followed by incubation for 2 hours. Cultures were spun at 5.000 g for 5 min and the supernatant filter-sterilized (0.2 μm), followed by dilution in SM buffer, titration on bacterial lawns of 8325-4 (TSB, 0.5 % agarose, 5 mM CaCl_2), and overnight incubation for determination of plaque forming units (PFU) ml^{-1} . The amount of phages produced per host cell was determined by calculating PFU ml^{-1} per CFU ml^{-1} .

Lysogenization frequency of ϕ 13

Exponential cultures of 8435-4 were infected with ϕ 13-kana at a MOI of 0.1 and 1. Phages were allowed to adsorb for 15 min on ice, after which cells were centrifuged and the pellet was resuspended in SM buffer. Dilutions were plated on TSA plates containing kanamycin for the determination of lysogens. Dilutions were further titrated on bacterial lawns of 8435-4 to detect cells in which the phage favored the lytic lifecycle. Phage titer was determined as PFU ml⁻¹ after overnight incubation. The lysogenization frequency was calculated as the ratio of lysogenic cells (CFU (Kan^R) ml⁻¹) of all infected cells (CFU (Kan^R) ml⁻¹ + PFU ml⁻¹).

RESULTS AND DISCUSSION

Topology of the ϕ 13 switch region and detection of identical switches in members of the Sa3int and the PVL encoding phages

Recently, a global search for DNA sequences similar to the phage TP901-1 switch region led us to identify a putative switch region in the *S. aureus* phage ϕ 13 (Pedersen *et al.*, 2020). As shown in the map in Fig. 1 and the amino acid sequence alignments in Appendix Fig. 2, the homology spans the N-terminal part of the *cl* gene, the intergenic region, and a divergently oriented, putative *mor* gene. Putative P_L and P_R promoters and O_R, O_L, and O_D operators were recognized in the ϕ 13 switch in similar locations as in TP901-1 (Pedersen *et al.*, 2020). The limited similarity was found to the C-terminal domain CI-CTD₁ from TP901-1, whereas the CI-CTD₂ showed no sign of conservation (Appendix Fig. 2). Instead of the CI-CTD₂ domain, the CI repressor from ϕ 13 carries a region with clear similarity to the C-terminal domain of the CI repressor from phage λ (see Appendix Fig. 2). The two catalytic residues from the peptidase domain as well as the autocatalytic site from λ are conserved in ϕ 13, suggesting that the CI repressor from ϕ 13, in contrast to the CI repressor from TP901-1 (Madsen *et al.*, 1999), could be capable of autocleavage.

To analyze if the ϕ 13 switch type was widespread among phages, we performed a homology search (Altschul *et al.*, 1990) with the 1260 bp ϕ 13 DNA sequence covering the region shown in Fig. 1,

1
2
3
4 excluding staphylococcal genome sequences. Only sequences from completed genomes of
5 staphylococcal phages were identified, and 6 phages had hits with full coverage and sequence
6 identity (>99% identity): PVL, tp301-1, P630, 3AJ-2017, IME1346_01, and ϕ 13. Two of these, 3AJ-
7 2017 and IME1346_01, encode the virulence proteins Sac, Chp, and Scn (Oliveira *et al.*, 2019) and
8 belong to the Sa3int group like ϕ 13, while the phages PVL and tp301-1 encoded the LukS-PV and
9 LukF-PV PVL virulence factors (Oliveira *et al.*, 2019). This shows that the homology between the
10 switches from ϕ 13 and TP901-1 is not unique and that the ϕ 13 switch type determines the decisions
11 between lysogenic and lytic growth for two important groups of phages carrying pathogenicity
12 genes.

ϕ 13 CI binds to operator sites in the intergenic region between *ci* and *mor*

21
22
23 To characterize the switch present in ϕ 13, it was first important to know that the postulated CI
24 repressor was functional and had an affinity towards the postulated CI operators. To determine
25 whether the CI repressor from ϕ 13 binds to these putative operators, CI was expressed with an N-
26 terminal His-TEV-tag (termed rCI, see Appendix Fig. 1) and purified by affinity chromatography and
27 gel filtration (Appendix Fig. 3A and B). After circular dichroism spectroscopy and differential
28 scanning fluorimetry had confirmed that the protein was folded and stable (Appendix Fig. 3C and
29 D), electrophoretic mobility shift assays (EMSA) were performed with this protein preparation using
30 fluorescent probes carrying O_R , O_L , or O_D from ϕ 13 (Fig. 2A). Agarose gel electrophoresis of binding
31 reactions with increasing CI concentration followed by detection of the labeled DNA by fluorescence
32 scanning showed that the rCI protein bound the O_L and O_D sites with high affinity (dissociation
33 constants of 22 nM and 15 nM, respectively), but with lower affinity to the O_R site (dissociation
34 constant of 310 nM) as shown in Fig. 2B and C. While the operator half-sites of the O_L and O_D
35 sequences correlated with the TP901-1 consensus (AGTTCAYR), one of the O_R half-sites deviated by
36 one base (AATTCATA). This difference could potentially explain the higher dissociation constant for
37 binding to O_R . To validate that the putative binding sites were responsible for the binding to rCI, a
38 series of mutated fluorescent DNA probes were produced, which were identical to the probes
39 shown in Fig. 2A, except that the central C nucleotide was mutated to G. Binding of rCI to these
40 mutated control probes was severely weakened and no bands for specific binding could be detected
41 (Fig. 2B).

1
2
3
4
5
6 Interestingly, it can be seen from Fig. 2B, that the bands with CI-bound DNA probe (marked with red
7 arrows) disappear at higher concentrations of CI. We hypothesize that this is due to multimerization
8 of CI because the labeled DNA probe migrates slowly as a smeared band at very high CI
9 concentrations (Lane 1 in all gels in Fig. 2B). To evaluate if the secondary binding events affected
10 the determination of the dissociation constants, we plotted the missing fraction of the free DNA
11 probe (i.e., the fraction of DNA probe that was retarded by any means) against the CI-concentration.
12 Using this quantification method, the apparent dissociation constants for CI binding to the O_L , O_D ,
13 and O_R probes were found to be 3.9 nM, 3.3 nM, and 100 nM, respectively (Fig. 2D), showing that
14 the secondary binding events affected the determination of the dissociation constants. Also, the Hill
15 coefficients for O_L and O_D binding were changed from 2.5 to 1.3 and 2.5 to 1.0 respectively (Fig. 2C).
16 The quantification of only the free DNA probe enabled the determination of apparent dissociation
17 constants for binding of CI to the negative controls. Dissociation constants were detected at
18 approximately 690 nM, 900 nM, and 690 nM, for the O_L^{control} , O_D^{control} , and O_R^{control} probes,
19 respectively, ten-fold and hundred-fold higher than the dissociation constants for the unmutated
20 probes. In combination, these results show that the CI repressor from $\phi 13$ is functional and that the
21 proposed operators are indeed binding sites for the repressor. The dissociation constants are
22 somewhat lower than for binding of TP901-1 CI to DNA containing TP901-1 operators, found by
23 mobility shift assays (Johansen, Brøndsted and Hammer, 2003; Pedersen and Hammer, 2008), but
24 recent mobility shift assays of TP901-1 CI binding to O_L using the same technique employed in this
25 study quantified the dissociation constant to 2.9 nM (Pedersen *et al.*, 2020). It is important to
26 mention that the binding of CI to O_R has introduced some interesting challenges. Preliminary
27 analysis of operator binding to the O_L , O_D , and O_R operators using purified CI, in which the His-TEV-
28 tag had been cleaved off, showed a dissociation constant that was slightly higher than shown above
29 for binding to probes containing the O_L and O_D operators (approximately 12 nM). Of more
30 importance, the binding of the O_R probe to this CI fraction showed dissociation constants equaling
31 the O_L and O_D operators (12 nM). This issue needs to be addressed in a future study, but the results
32 obtained here and presented in Fig. 2 have established that the proposed O_L , O_D , and O_R operators
33 are specific binding sites for the $\phi 13$ CI repressor.
34
35
36
37
38
39
40
41
42
43
44
45
46
47
48
49
50
51
52
53
54
55
56
57
58
59
60

A minimal 1.3 kb switch region from ϕ 13 is capable of decision switching in *S. aureus*

After having shown that the *cl* encoded repressor can bind to an operator (O_L) overlapping the putative P_L promoter as in the TP901-1 switch, the isolation of a functional ϕ 13 switch for *in vivo* analysis of switch frequencies appeared to be feasible. Previously a DNA fragment spanning the *cl* and *mor* genes from TP901-1 had successfully been inserted into a promoter fusion plasmid (Madsen *et al.*, 1999), and used for detailed characterization of the TP901-1 switch (Pedersen and Hammer, 2008) through transformation of its *L. lactis* host. To monitor the regulatory decisions upon introduction of ϕ 13 switch DNA, we constructed plasmids with transcriptional fusions to the P_L promoter of the ϕ 13 switch region, as illustrated in Fig. 3, with a *lacZ* reporter gene located after the *mor* gene. Upon transformation and plating on selective plates containing X-gal, the resulting colonies were either blue, indicative of high *mor* expression from the lytic P_L promoter, referred to as the “lytic” phenotype, or white, indicative of low *mor* expression due to repression of the P_L promoter by CI expressed from the lysogenic P_R promoter, referred to as the “lysogenic” phenotype.

Plasmid pCSK3 replicates in *S. aureus* and upon transformation of strain 8325-4 with pCSK3 we observed an average of 4.8 % transformants with the “lysogenic” colony phenotype and 95 % with the “lytic” phenotype (Table 4). This result indicated that the switch region present in pCSK3 could indeed perform decision switching in *S. aureus*. The genetic integrity of the switch region was verified by purification and subsequent re-transformation of pCSK3 isolated from 8325-4/pCSK3 transformants, yielding similar decision frequencies (see footnote to Table 4). Since the decision analysis was performed using a plasmid and not an intact phage, the use of pCSK3 as a model system for the ϕ 13 decision switching required that the frequency of the “lysogenic” phenotype reflected the true lysogenization frequency. Infection of strain 8325-4 with the ϕ 13-kana phage was therefore performed at a MOI of 1 and 0.1 at a bacterial concentration of 1.3×10^8 CFU ml⁻¹. As shown in Appendix Table 3, the average lysogenization frequency from five replicates was $4.6 \% \pm 2.8 \%$ and $3.5 \% \pm 3.3 \%$ for infections at an MOI of 1, and 0.1, respectively. Since the pCSK3 “lysogenic” (4.9 %) and ϕ 13 lysogenic frequencies are not significantly different ($p=0.87$ and 0.47 , for the two MOIs, respectively), we believe that the pCSK3 switch plasmid is a faithful biological model for ϕ 13 switching. Finally, to ensure the importance of the MOR protein for the lytic pathway of the ϕ 13 decision process, the start-codon in the *mor* gene was changed to a stop codon. The resulting

1
2
3
4 plasmids, pCSK12, and pCSK13 acquired the “lysogenic” phenotype in 100 % of transformations
5
6 when introduced into *S. aureus* 8325-4, showing that the “lytic” phenotype is dependent upon the
7
8 MOR protein (Appendix Table 4).
9

10
11 To analyze whether the decision frequency of the ϕ 13 switch was dependent upon replication of
12
13 the plasmid containing the switch DNA during the decision process, we introduced the switch on an
14
15 integrative plasmid, pCSK9. Plasmid integration occurs at the bacterial attachment site of the phage
16
17 L54a located in the lipase gene *geh* of *S. aureus* and is catalyzed by the phage integrase provided by
18
19 plasmid pYL112-19 (Luong and Lee, 2007). Transformation of *S. aureus* 8325-4 with pCSK9 yielded a
20
21 higher number of “lysogenic” colonies than with pCSK3 (12 % compared to 4.9 %, see Table 4).
22
23 However, the very low efficiency of transformation (in total 77 transformants from 5 individual
24
25 transformations) resulted in a high degree of variation, preventing a reliable determination of the
26
27 decision frequency. Despite this, the transformations permitted the isolation of pCSK9
28
29 transformants with both the “lysogenic” (CSK48) and “lytic” (CSK47) colony phenotype.
30
31

32 ***The “lysogenic” colony phenotype from switch plasmids confers ϕ 13 immunity***

33 To assess whether the “lysogenic” colony phenotype expressed from the switch plasmids was
34
35 functionally equivalent with the immunity derived from the ϕ 13 prophages, we first tested if a ϕ 13
36
37 lysogen could influence the decision frequency of the switch plasmids. To this end, pCSK3 and pCSK9
38
39 were introduced by transformation into (immune) *S. aureus* carrying a fully functional derivative of
40
41 ϕ 13 containing a kanamycin resistance gene (8325-4 ϕ 13-kana) integrated into the chromosome
42
43 (Tang *et al.*, 2017). Despite a small number of successful transformation events (63 transformants
44
45 from 9 individual transformations), which prevented reliable quantification of the switching
46
47 frequency, it was striking that we exclusively observed “lysogenic” transformants when the ϕ 13-
48
49 kana lysogen was transformed with pCSK9 (Table 4, column 4), suggesting that the production of CI
50
51 by the ϕ 13 lysogen had influenced the decision process by pCSK9. Accordingly, the vast majority
52
53 (99.6 %) of pCSK3 transformants of *S. aureus* 8425-4 ϕ 13-kana were “lysogenic” on X-gal-containing
54
55 plates, showing a strong influence of lysogenic levels of CI on the decision by pCSK3. Interestingly, a
56
57 small fraction of 0.4 % established the “lytic” phenotype despite the presence of the ϕ 13 prophage,
58
59 verified by PCRs and kanamycin resistance. To analyze whether the switch or the reporter gene had
60

1
2
3
4 mutated, plasmids were purified from the colonies that had escaped the immunity phenotype.
5
6 Transformation of these plasmids into 8325-4 with and without the ϕ 13 prophage yielded decision
7
8 frequencies similar to the original transformations (see footnote to Table 4), showing that the “lytic”
9
10 colony phenotype was not a result of mutations.
11

12
13 We then investigated whether the plasmid-derived “lysogenic” phenotype could confer ϕ 13
14
15 immunity upon infection (Fig. 4). When a liquid culture of the “lysogenic” 8325-4/pCSK3 (CSK33)
16
17 was infected with ϕ 13-kana, the “lysogenic” phenotype was found to restrict the production of
18
19 phages (compare B and E in Fig. 4). The same result was found when a transformant carrying the
20
21 integrated pCSK9 plasmid (8325-4 *geh*::pCSK9, CSK48) was inoculated from a “lysogenic” colony and
22
23 was infected with ϕ 13-kana (compare A and C in Fig. 4), showing that CI expressed from a
24
25 chromosomally integrated ϕ 13 switch conferred immunity to attacking ϕ 13 phages. When cells with
26
27 the integrated switch plasmid were inoculated from a “lytic” colony and infected with ϕ 13, the
28
29 presence of the switch did not affect phage production (compare A and D in Fig. 4). Surprisingly,
30
31 however, when cells containing the replicative plasmid pCSK3 were inoculated from a “lytic” colony
32
33 and infected by ϕ 13-kana, the “lytic” switch phenotype inhibited phage production (compare B and
34
35 F in Fig. 4). It has previously been shown that replicating switch plasmids of TP901-1 favoring P_L
36
37 (“lytic” phenotype) resulted in partial immunity towards infecting phages (Madsen *et al.*, 1999), in
38
39 accordance with the present results. This suggests that, although there is not enough CI repressor
40
41 present to repress P_L on the multi-copy switch plasmid, the concentration is still sufficient to prevent
42
43 lytic phage development. Upon screening of kanamycin resistance in cells surviving ϕ 13-kana
44
45 infection, very few lysogenic cells were detected, showing that survival under these conditions is
46
47 not due to the formation of ϕ 13-kana lysogens. Thus, the multi-copy plasmid-derived “lytic” switch
48
49 phenotype appears to inactivate phage development in either direction.
50

Decision switching by the minimal switch region from ϕ 13 does not require *S. aureus* host factors

51
52 As *E. coli* host factors are known to affect the integration and induction of phage λ (Roucourt and
53
54 Lavigne, 2009), it was of interest to establish whether the ϕ 13 switch can function independently
55
56 of host factors. Switch plasmid pCSK3 has an origin of replication that is functional in most Gram-
57
58 positive bacteria (Kovács *et al.*, 2010), and we could therefore also examine ϕ 13 switching in *Bacillus*
59
60

1
2
3
4
5
6
7
8
9
10
11
12
13
14
15
16
17
18
19
20
21
22
23
24
25
26
27
28
29
30
31
32
33
34
35
36
37
38
39
40
41
42
43
44
45
46
47
48
49
50
51
52
53
54
55
56
57
58
59
60

subtilis. As *B. subtilis* is a heterologous host, it carries no specific staphylococcal factors but contains general Gram-positive host factors. Upon transformation of pCSK3 into *B. subtilis* 168, we observed an average frequency of “lysogenic” colonies of 2-3 % (Table 4), which is close to the frequency obtained in *S. aureus*. This suggested that the decision frequency was not affected by specific host factors.

Low spontaneous induction frequency from the “lysogenic” phenotype to the “lytic” phenotype

To examine the stability of the ϕ 13 “lysogenic” colony switch phenotype, simulating the stability of ϕ 13 lysogenic cells, we suspended and plated a large number of cells from “lysogenic” colonies on agar plates containing X-gal. Around 0.2 % “lytic” colonies were detected in otherwise “lysogenic” colonies from both *B. subtilis* and *S. aureus*. This low level of toggling from the “lysogenic” to the “lytic” colony phenotype is hypothesized to be due to spontaneous induction of the SOS response, which is inevitable and leads to prophage induction in bacteria that contain an SOS response and an intact *recA* gene (Goerke, Koller and Wolz, 2006). To distinguish the process of toggle switching from a mutational event leading to the “lytic” colony phenotype, we purified pCSK3 plasmid from “lytic” spontaneous revertants and re-transformed them into the same host, with and without the ϕ 13 prophage. After transformation of the strains with the extracted pCSK3 plasmid, we obtained a frequency of “lysogenic” transformant colonies at 5 % for re-transformation of 8325-4, and at 100 % for re-transformation 8325-4 ϕ 13 kana, indistinguishable from frequencies obtained by transformation with the original plasmid, and showing that the change was epigenetic rather than mutational.

High toggle frequency of the ϕ 13 switch from the “lytic” to the “lysogenic” phenotype

While the “lysogenic” colony phenotype was very stable, the “lytic” colony phenotype was subject to frequent toggling to the “lysogenic” phenotype. When the cells from small (young) “lytic” colonies were suspended in medium and plated on agar plates containing X-gal, around 3 % of the colonies had assumed the “lysogenic” phenotype. Plating of larger (older) “lytic” colonies resulted in an average of 60 % “lysogenic” colonies. Because of the highly artificial nature of the “lytic” phenotype, the stability of the phenotype was not analyzed further.

Induction of the “lytic” switch phenotype by DNA damaging agents

Above, we reported that 0.2 % of cells that had grown in “lysogenic” colonies on an agar plate had spontaneously toggled to the “lytic” phenotype, possibly initiated by the spontaneous induction of the SOS response. A more dramatic visualization of the interplay between the DNA damage and the $\phi 13$ switch could be observed by exposing “lysogenic” cells to a gradient of DNA damaging agents on agar plates containing X-gal. Induction of “lysogenic” (white) to “lytic” (blue) toggle switching is intimately connected to the level of the DNA damaging compound as seen in Fig. 5. In our working hypothesis, the cellular CI concentration is determined through a race between CI expression and CI degradation, where a threshold CI concentration has to be crossed if the switch should toggle from the “lysogenic” to the “lytic” phenotype. Two clear zones can be detected among the bacterial colonies on the X-gal-containing plates at different distances from the DNA damaging agents: a death zone and a toggle-inducing zone. The minimal inhibitory concentration (MIC) of the DNA damaging agent must be located at the border between growth and non-growth. Accordingly, a minimal toggle-inducing concentration (MTC) can be located at the border between purely white colonies and colonies with a bluish tint. For this analysis, a suspension of bacteria with the “lysogenic” (white) phenotype was plated on agar plates, and a drop of DNA damaging agent was applied to the center. Mitomycin C, ciprofloxacin, and hydrogen peroxide are all known to induce $\phi 13$ lysogens (Goerke, Koller, and Wolz, 2006; Tang *et al.*, 2017), and Fig. 5 shows the response of the $\phi 13$ switch plasmid to gradients of DNA damaging agents in its natural host (Fig. 5, left panel, 8325-4 *geh::pCSK9* (CSK48)) and in *B. subtilis* (Fig. 5, right panel, 168 *thrC::pCSK2* (CSK9)). In all cases, a sharp boundary (MIC) was formed, where no cells could grow inside the boundary, but where colonies could be formed in the sub-MIC concentrations outside the boundary.

Mitomycin C and ciprofloxacin exposure resulted in very similar induction patterns in both *S. aureus* and *B. subtilis* hosts. The colony phenotypes showed a wide toggle-inducing zone where a varying fraction of cells had switched to a “lytic” (blue) phenotype (top four panels in Fig. 5). Hydrogen peroxide showed an extremely thin toggle-inducing zone for the *S. aureus* host but no toggle-inducing zone at all for the *B. subtilis* host (bottom panels in Fig. 5). The difference in induction pattern most likely reflects that the MTC for hydrogen peroxide is higher than the MIC value in *B.*

1
2
3
4 *subtilis*, but that MTC and MIC are almost equal in *S. aureus*. For mitomycin C and ciprofloxacin, the
5 MTC value is significantly lower than the MIC value in both hosts.
6
7

8
9
10 Across the toggle-inducing zone of mitomycin C and ciprofloxacin the intensity of blue color
11 decreases (top four panels in Fig. 5), likely due to smaller fractions of toggle-switched cells in the
12 colonies. To quantify the fractions of stable toggle-switched cells, we picked colonies grown at
13 known distances from an application spot containing mitomycin C and determined the fraction of
14 cells in each colony that could form colonies with a stable “lytic” phenotype. After a suspension of
15 each colony in a fresh medium, plating, incubation, and quantifying the fraction of “lytic” colonies,
16 an exponential dependency was observed between the frequency of “lytic” cells and the distance
17 to the application spot for both *S. aureus* and *B. subtilis* (Fig. 6). This could suggest a quasi-linear
18 dependence between the toggle switch frequency and the mitomycin C concentration since we
19 expect a similar decrease in concentration by diffusion of a compound in agar (Koch, 1999), although
20 the inherent instability of the “lytic” phenotype detected above should be taken into consideration.
21 This dependence of toggle frequency on the concentration of the DNA damaging agent suggests the
22 existence of high stochasticity in either the level of DNA damage, the concentration of RecA*
23 nucleofilaments, the rate of autocleavage of CI, or the competition between the elements in the
24 $\phi 13$ switch. Experiments to unravel the kinetic relationship between induction of the SOS response
25 and the toggle switching of the genetic switch would be interesting, but it would require
26 simultaneous monitoring of the SOS response.
27
28
29
30
31
32
33
34
35
36
37
38
39
40
41
42

43 **Timing of commitment to the “lytic” phenotype in *S. aureus***

44 To examine the timing of the response of the switch to DNA damage, we exposed “lysogenic” 8325-4
45 *geh::pCSK9* (CSK48) cells to mitomycin C at a final concentration of 1 $\mu\text{g ml}^{-1}$. Induction of toggle
46 switch to the “lytic” phenotype was monitored by plating dilutions of the mitomycin C treated
47 culture on TSA plates containing X-gal. A “lytic” phenotype indicated that the induced cell that
48 formed the colony was committed to the “lytic” phenotype and had passed on the phenotype to
49 the descendants in the colony. Figure 7 shows the temporal increase in the fraction of cells
50 committed to forming colonies with a stable “lytic” phenotype (in %). The highest frequency of
51 commitment to the “lytic” phenotype was obtained between 5 and 40 min of exposure to mitomycin
52
53
54
55
56
57
58
59
60

1
2
3
4 C, and as many as 30 % of all cells became dedicated in 20 to 30 min. However, because of the
5 stochastic nature of the induction process, a fraction of the bacteria showed commitment in less
6 than 5 min of exposure to mitomycin C (3 % of the cells), while other cells required exposure for
7 more than 40 min before commitment (10 % of the cells). As discussed above, the CI threshold
8 allowing toggle switching is determined by many factors, such as the extent of DNA damage, the CI
9 degradation rate, the CI synthesis rate, and $\phi 13$ switch kinetics, each adding to the overall
10 stochasticity of the process.
11
12
13
14
15
16
17
18

19 CONCLUSIONS

20
21
22 In this study, we have reported the first analysis of a genetic switch from a Sa3int bacteriophage
23 with implications for the phage-derived host specificity of *S. aureus* bacteria towards humans. As
24 identical switches are present in other Sa3int phages and unrelated phages carrying genes for PVL,
25 the results are also relevant for a larger group of pathogenic phages. Inhibition of the process
26 leading to phage integration into *S. aureus* hosts could influence their ability to colonize humans.
27 Therefore, it is crucial to understand the process by which the phage switch decides between i)
28 lysogenization of the host to integrate as a prophage or ii) multiplying and killing of the host. It is
29 equally important to understand the toggle process that induces a Sa3int prophage to kill the
30 bacterium and release a litter of newly produced phages. We have shown that a minimal genetic
31 switch of $\phi 13$, contained on a 1.3 kb DNA fragment and expressing functional *ci* and/or *mor* genes
32 from divergent promoters, is fully competent in both decision switching and toggle switching.
33 Purified his-tagged CI protein was found to be folded, stable, and to bind with high affinity to
34 operators with two half-sites following the AGTTCAYR consensus, but with low affinity to mutant
35 operators (AGTTGAYR). The two alternative phenotypes of the epigenetic switch are not equally
36 stable. While the “lysogenic” phenotype is very stable (although chosen in less than 5% of the
37 decision events) and leads to the lysogenic life cycle of the phage, the frequent “lytic” phenotype
38 that resembles the first phase in the lytic life cycle is unstable and toggles towards the “lysogenic”
39 phenotype. If this high toggle frequency indicates that prophage induction may be reversible in its
40 early phase, then our preliminary findings that the nutritional status of the cell can modulate the
41 toggle frequency could prove relevant.
42
43
44
45
46
47
48
49
50
51
52
53
54
55
56
57
58
59
60

1
2
3
4
5
6 Induction of “lysogenic” to “lytic” toggling by DNA damaging agents, resembling the induction of
7 the $\phi 13$ prophage, was visualized in a plate diffusion assay that enabled us to locate MIC and MTC
8 (minimal toggle-inducing concentration) values (Fig. 5). In this work, we defined MTC values as a
9 tool to distinguish between the antibiotic killing of cells by inhibition of cell function from killing by
10 induction of phage lysis. Relative MIC/MTC ratios could be important in the clinical use of DNA
11 damaging antibiotics to prevent phage lysis mediated toxin production (Zhang *et al.*, 2000) or
12 production of host transforming phages like $\phi 13$. Antibiotics with a MIC/MTC ratio below 1.0 would
13 be safe in this regard; however, as shown for hydrogen peroxide (Fig. 5), the MIC/MTC ratio can be
14 strain or species-specific. Timing of the induction process revealed a highly stochastic process with
15 a maximal toggling rate, leading to dedicated cells with the stable “lytic” phenotype, between 20
16 and 30 min of exposure to mitomycin C. While the induction of DNA damage in each cell ultimately
17 defines a particular CI degradation rate, this could easily be changing over time due to the SOS
18 induction of DNA repair enzymes. The stochasticity of the toggle frequency at different time points
19 could originate at many levels, including the initial CI and MOR concentrations, their production
20 levels, and the DNA damage-induced CI degradation rate. While toggle switching has been reported
21 for many bistable switches (Dubnau and Losick, 2006), the ability of an isolated switch to conduct
22 both decision switching and toggle switching has not previously been demonstrated for any phage.
23
24
25
26
27
28
29
30
31
32
33
34
35
36
37
38

39 **DATA AVAILABILITY STATEMENT**

40 The data generated and analyzed during the current study are available in the Zenodo repository at
41 <https://doi.org/10.5281/zenodo.5515850>
42
43
44
45

46 **AUTHOR CONTRIBUTIONS**

47 Camilla Kristensen

48 Conceptualization-Equal, Data curation-Lead, Investigation-Lead, Methodology-Equal, Validation-
49 Equal, Visualization-Equal, Writing-original draft-Equal, Writing-review & editing-Equal
50
51

52 Anders Varming

53 Data curation-Supporting, Formal analysis-Supporting, Investigation-Supporting, Writing-review &
54 editing-Equal
55
56

57 Helena Leinweber
58
59
60

1
2
3
4 Investigation-Supporting, Supervision-Supporting, Writing-review & editing-Equal
5

6
7 Karin Hammer

8 Conceptualization-Supporting, Methodology-Supporting, Validation-Supporting, Writing-original
9 draft-Supporting, Writing-review & editing-Equal
10

11
12 Leila Lo Leggio

13 Conceptualization-Supporting, Data curation-Supporting, Formal analysis-Supporting, Funding
14 acquisition-Equal, Methodology-Supporting, Supervision-Supporting, Validation-Supporting,
15 Writing-original draft-Supporting, Writing-review & editing-Equal
16

17
18 Hanne Ingmer

19 Conceptualization-Supporting, Funding acquisition-Equal, Supervision-Equal, Writing-original draft-
20 Supporting, Writing-review & editing-Equal
21

22
23 Mogens Kilstrup

24 Conceptualization-Lead, Data curation-Equal, Investigation-Equal, Methodology-Equal, Project
25 administration-Lead, Supervision-Lead, Visualization-Equal, Writing-original draft-Equal, Writing-
26 review & editing-Equal
27

28 29 **ACKNOWLEDGEMENTS**

30
31 We thank associate professor Peter W. Thulstrup from the University of Copenhagen for access to
32 the CD spectropolarimeter. A.K.V. is funded by a Ph.D. scholarship from the Lundbeck Foundation
33 (grant R249-2017-977). H.L. was funded from the European Union's Horizon 2020 research and
34 innovation program under the Marie Skłodowska-Curie grant agreement no. 765147.
35
36
37
38
39

40 **CONFLICT OF INTEREST**

41
42 None declared.
43
44

45 **ETHICS STATEMENT**

46
47 None required.
48
49
50
51
52
53
54
55
56
57
58
59
60

REFERENCES

- Altschul, S. F. *et al.* (1990) 'Basic local alignment search tool', *Journal of Molecular Biology*. *J Mol Biol*, 215(3), pp. 403–410. doi: 10.1016/S0022-2836(05)80360-2.
- Atsumi, S. and Little, J. W. (2006) 'Role of the lytic repressor in prophage induction of phage λ as analyzed by a module-replacement approach', *Proceedings of the National Academy of Sciences of the United States of America*. National Academy of Sciences, 103(12), pp. 4558–4563. doi: 10.1073/pnas.0511117103.
- Burkholder, P. R. and Giles, N. H. (1947) 'Induced biochemical mutations in *Bacillus subtilis*', *American journal of botany*, 34(6), pp. 345–348. doi: 10.2307/2437147.
- Casjens, S. R. and Hendrix, R. W. (2015) 'Bacteriophage lambda: Early pioneer and still relevant', *Virology*. Academic Press Inc., pp. 310–330. doi: 10.1016/j.virol.2015.02.010.
- Coleman, D. *et al.* (1991) 'Insertional inactivation of the *Staphylococcus aureus* β -toxin by bacteriophage ϕ 13 occurs by site- and orientation-specific integration of the ϕ 13 genome', *Molecular Microbiology*, 5(4), pp. 933–939. doi: 10.1111/j.1365-2958.1991.tb00768.x.
- Dubnau, D. and Losick, R. (2006) 'Bistability in bacteria', *Molecular Microbiology*. *Mol Microbiol*, pp. 564–572. doi: 10.1111/j.1365-2958.2006.05249.x.
- Gardner, T. S., Cantor, C. R. and Collins, J. J. (2000) 'Construction of a genetic toggle switch in *Escherichia coli*', *Nature*. Nature Publishing Group, 403(6767), pp. 339–342. doi: 10.1038/35002131.
- Gasteiger, E. *et al.* (2005) 'Protein Identification and Analysis Tools on the ExPASy Server', *The Proteomics Protocols Handbook*, pp. 571–608. doi: 10.1385/1592598900.
- Ghodke, H. *et al.* (2019) 'Spatial and temporal organization of reca in the escherichia coli dna-damage response', *eLife*. eLife Sciences Publications Ltd, 8. doi: 10.7554/ELIFE.42761.
- Goerke, C. *et al.* (2006) 'Extensive phage dynamics in *Staphylococcus aureus* contributes to adaptation to the human host during infection', *Molecular Microbiology*, 61(6), pp. 1673–1685. doi: 10.1111/j.1365-2958.2006.05354.x.
- Goerke, C. *et al.* (2009) 'Diversity of Prophages in Dominant *Staphylococcus aureus* Clonal Lineages', *Journal of Bacteriology*, 191(11), pp. 3462 LP – 3468. doi: 10.1128/JB.01804-08.
- Goerke, C., Koller, J. and Wolz, C. (2006) 'Ciprofloxacin and Trimethoprim Cause Phage Induction and Virulence Modulation in *Staphylococcus aureus*', *Antimicrobial Agents and Chemotherapy*,

1
2
3
4 50(1), pp. 171–177. doi: 10.1128/AAC.50.1.171-177.2006.

6 Grodzicker, T., Arditti, R. R. and Eisen, H. (1972) 'Establishment of repression by lambdoid phage in
7 catabolite activator protein and adenylate cyclase mutants of *Escherichia coli.*', *Proceedings of the*
8 *National Academy of Sciences of the United States of America*. National Academy of Sciences,
9
10 69(2), pp. 366–370. doi: 10.1073/pnas.69.2.366.

13 Guérout-Fleury, A. M., Frandsen, N. and Stragier, P. (1996) 'Plasmids for ectopic integration in
14 *Bacillus subtilis*', *Gene*. Elsevier, 180(1–2), pp. 57–61. doi: 10.1016/S0378-1119(96)00404-0.

17 Herman, C. *et al.* (1993) 'Cell growth and λ phage development controlled by the same essential
18 *Escherichia coli* gene, *ftsH/hflB*', *Proceedings of the National Academy of Sciences of the United*
19 *States of America*, 90(22), pp. 10861–10865. doi: 10.1073/pnas.90.22.10861.

22 Huseby, M. *et al.* (2007) 'Structure and biological activities of beta toxin from *Staphylococcus*
23 *aureus*', *Journal of Bacteriology*, 189(23), pp. 8719–8726. doi: 10.1128/JB.00741-07.

26 Ingmer, H., Gerlach, D. and Wolz, C. (2019) 'Temperate Phages of *Staphylococcus aureus*',
27 *Microbiology Spectrum*, 7(5). doi: 10.1128/microbiolspec.gpp3-0058-2018.

29 Johansen, A. H., Brøndsted, L. and Hammer, K. (2003) 'Identification of operator sites of the CI
30 repressor of phage TP901-1: Evolutionary link to other phages', *Virology*. Academic Press Inc.,
31 311(1), pp. 144–156. doi: 10.1016/S0042-6822(03)00169-7.

33 Katayama, Y. *et al.* (2013) 'Beta-hemolysin promotes skin colonization by *Staphylococcus aureus*',
34 *Journal of Bacteriology*, 195(6), pp. 1194–1203. doi: 10.1128/JB.01786-12.

37 Kihara, A., Akiyama, Y. and Ito, K. (2001) 'Revisiting the lysogenization control of bacteriophage λ .
38 Identification and characterization of a new host component, HflD', *Journal of Biological*
39 *Chemistry*. American Society for Biochemistry and Molecular Biology Inc., 276(17), pp. 13695–
40 13700. doi: 10.1074/jbc.M011699200.

42 Koch, A. L. (1999) 'Diffusion through agar blocks of finite dimensions: A theoretical analysis of
43 three systems of practical significance in microbiology', *Microbiology*. Society for General
44 Microbiology, 145(3), pp. 643–654. doi: 10.1099/13500872-145-3-643.

46 Konkol, M. A., Blair, K. M. and Kearns, D. B. (2013) 'Plasmid-encoded ComI inhibits competence in
47 the ancestral 3610 strain of *Bacillus subtilis*', *Journal of Bacteriology*. American Society for
48 Microbiology Journals, 195(18), pp. 4085–4093. doi: 10.1128/JB.00696-13.

51 Kovács, Á. T. *et al.* (2010) 'Genetic tool development for a new host for biotechnology, the
52
53
54
55
56
57
58
59
60

1
2
3
4 thermotolerant bacterium *Bacillus coagulans*', *Applied and Environmental Microbiology*, 76(12),
5 pp. 4085–4088. doi: 10.1128/AEM.03060-09.

6
7
8 Lee, C. Y., Buranen, S. L. and Zhi-Hai, Y. (1991) 'Construction of single-copy integration vectors for
9 *Staphylococcus aureus*', *Gene*, 103(1), pp. 101–105. doi: 10.1016/0378-1119(91)90399-V.

10
11 Little, J. W. (1984) 'Autodigestion of *lexA* and phage λ repressors', *Proceedings of the National*
12 *Academy of Sciences of the United States of America*. National Academy of Sciences, 81(3 1), pp.
13 1375–1379. doi: 10.1073/pnas.81.5.1375.

14
15
16
17 Liu, G. Y. (2009) 'Molecular pathogenesis of *Staphylococcus aureus* infection', *Pediatric Research*.
18 NIH Public Access, p. 71R. doi: 10.1203/PDR.0b013e31819dc44d.

19
20
21 Lowy, F. D. (1998) '*Staphylococcus aureus* Infections', *New England Journal of Medicine*.
22 Massachusetts Medical Society, 339(8), pp. 520–532. doi: 10.1056/NEJM199808203390806.

23
24 Luong, T. T. and Lee, C. Y. (2007) 'Improved single-copy integration vectors for *Staphylococcus*
25 *aureus*', *Journal of Microbiological Methods*, 70(1), pp. 186–190. doi:
26
27 10.1016/j.mimet.2007.04.007.

28
29
30 Madsen, P. L. *et al.* (1999) 'The genetic switch regulating activity of early promoters of the
31 temperate lactococcal bacteriophage TP901-1', *Journal of Bacteriology*. American Society for
32 Microbiology, 181(24), pp. 7430–7438. doi: 10.1128/jb.181.24.7430-7438.1999.

33
34
35 Micsonai, A. *et al.* (2015) 'Accurate secondary structure prediction and fold recognition for circular
36 dichroism spectroscopy', *Proceedings of the National Academy of Sciences of the United States of*
37 *America*. National Academy of Sciences, 112(24), pp. E3095–E3103. doi:
38
39 10.1073/pnas.1500851112.

40
41
42
43 Micsonai, A. *et al.* (2018) 'BeStSel: A web server for accurate protein secondary structure
44 prediction and fold recognition from the circular dichroism spectra', *Nucleic Acids Research*.
45 Oxford University Press, 46(W1), pp. W315–W322. doi: 10.1093/nar/gky497.

46
47
48 Monk, I. R. *et al.* (2015) 'Complete bypass of restriction systems for major *Staphylococcus aureus*
49 lineages', *mBio*, 6(3), pp. 1–12. doi: 10.1128/mBio.00308-15.

50
51
52 Novick, R. (1967) 'Properties of a cryptic high-frequency transducing phage in *Staphylococcus*
53 *aureus*', *Virology*. Academic Press, 33(1), pp. 155–166. doi: 10.1016/0042-6822(67)90105-5.

54
55
56
57 Novick, R. P. (1963) 'Analysis by transduction of mutations affecting penicillinase formation',
58 *Journal of general microbiology*, 33(1), pp. 121–136. doi: 10.1099/00221287-33-1-121.

- 1
2
3
4 Oppenheim, A. B. *et al.* (2005) 'Switches in Bacteriophage Lambda Development', *Annual Review*
5 *of Genetics*. Annual Reviews, 39(1), pp. 409–429. doi: 10.1146/annurev.genet.39.073003.113656.
6
7
8 Pedersen, M. *et al.* (2020) 'Repression of the lysogenic PR promoter in bacteriophage TP901-1
9 through binding of a CI-MOR complex to a composite OM-OR operator', *Scientific Reports*, 10(1),
10 p. 8659. doi: 10.1038/s41598-020-65493-0.
11
12
13 Pedersen, M. and Hammer, K. (2008) 'The Role of MOR and the CI Operator Sites on the Genetic
14 Switch of the Temperate Bacteriophage TP901-1', *Journal of Molecular Biology*. Elsevier BV,
15 384(3), pp. 577–589. doi: 10.1016/j.jmb.2008.09.071.
16
17
18 Riva, S., Polsinelli, M. and Falaschi, A. (1968) 'A new phage of *Bacillus subtilis* with infectious DNA
19 having separable strands', *Journal of Molecular Biology*. Academic Press, 35(2), pp. 347–356. doi:
20 10.1016/S0022-2836(68)80029-4.
21
22
23 Roucourt, B. and Lavigne, R. (2009) 'The role of interactions between phage and bacterial proteins
24 within the infected cell: a diverse and puzzling interactome', *Environmental Microbiology*, 11(11),
25 pp. 2789–2805. doi: 10.1111/j.1462-2920.2009.02029.x.
26
27
28 Salgado-Pabón, W. *et al.* (2014) '*Staphylococcus aureus* β -toxin production is common in strains
29 with the β -toxin gene inactivated by bacteriophage', *Journal of Infectious Diseases*, 210(5), pp.
30 784–792. doi: 10.1093/infdis/jiu146.
31
32
33 Schindelin, J. *et al.* (2012) 'Fiji: an open-source platform for biological-image analysis', *Nature*
34 *Methods* 2012 9:7. Nature Publishing Group, 9(7), pp. 676–682. doi: 10.1038/nmeth.2019.
35
36
37 Shao, Q., Trinh, J. T. and Zeng, L. (2019) 'High-resolution studies of lysis–lysogeny decision-making
38 in bacteriophage lambda', *Journal of Biological Chemistry*, 294(10), pp. 3343–3349. doi:
39 10.1074/jbc.TM118.003209.
40
41
42
43 Sreerama, N. and Woody, R. W. (2000) 'Estimation of protein secondary structure from circular
44 dichroism spectra: Comparison of CONTIN, SELCON, and CDSSTR methods with an expanded
45 reference set', *Analytical Biochemistry*, 287(2), pp. 252–260. doi: 10.1006/abio.2000.4880.
46
47
48 Tang, Y. *et al.* (2017) 'Commercial biocides induce transfer of prophage Φ 13 from human strains of
49 *Staphylococcus aureus* to livestock CC398', *Frontiers in Microbiology*. Frontiers Media S.A., 8(Dec),
50 p. 2418. doi: 10.3389/fmicb.2017.02418.
51
52
53
54
55 Tong, S. Y. C. *et al.* (2015) '*Staphylococcus aureus* infections: Epidemiology, pathophysiology,
56 clinical manifestations, and management', *Clinical Microbiology Reviews*. American Society for
57
58
59
60

1
2
3
4
5
6
7
8
9
10
11
12
13
14
15
16
17
18
19
20
21
22
23
24
25
26
27
28
29
30
31
32
33
34
35
36
37
38
39
40
41
42
43
44
45
46
47
48
49
50
51
52
53
54
55
56
57
58
59
60

Microbiology, 28(3), pp. 603–661. doi: 10.1128/CMR.00134-14.

Whitmore, L. and Wallace, B. A. (2008) 'Protein secondary structure analyses from circular dichroism spectroscopy: Methods and reference databases', *Biopolymers*. *Biopolymers*, 89(5), pp. 392–400. doi: 10.1002/bip.20853.

Xia, G. and Wolz, C. (2014) 'Phages of *Staphylococcus aureus* and their impact on host evolution', *Infection, Genetics and Evolution*. Elsevier, 21, pp. 593–601. doi: 10.1016/j.meegid.2013.04.022.

Zhang, X. *et al.* (2000) 'Quinolone Antibiotics Induce Shiga Toxin–Encoding Bacteriophages, Toxin Production, and Death in Mice', *The Journal of Infectious Diseases*. Oxford Academic, 181(2), pp. 664–670. doi: 10.1086/315239.

CONFIDENTIAL - DO NOT DISTRIBUTE

TABLES

Table 1. List of selected bacterial strains used in this study. Strain, species, a short description, and reference of selected strains. See Appendix Table 1 for a complete list.

Strain	Species	Short description or relevant genotype	Reference or source
168	<i>B. subtilis</i>		(Burkholder and Giles, 1947)
8325-4	<i>S. aureus</i>	NCTC8325 phage cured	(Novick, 1967)
8325-4 ϕ 13-kana	<i>S. aureus</i>	8325-4 lysogenized with ϕ 13-kana	(Tang <i>et al.</i> , 2017)
CSK8	<i>B. subtilis</i>	168 <i>thrC</i> ::pCSK2 expressing the “lytic” phenotype	This study
CSK9	<i>B. subtilis</i>	168 <i>thrC</i> ::pCSK2 expressing the “lysogenic” phenotype	This study
CSK10	<i>B. subtilis</i>	168/pCSK3 expressing the “lytic” phenotype	This study
CSK11	<i>B. subtilis</i>	168/pCSK3 expressing the “lysogenic” phenotype	This study
CSK32	<i>S. aureus</i>	8325-4/pCSK3 expressing the “lytic” phenotype	This study
CSK33	<i>S. aureus</i>	8325-4/pCSK3 expressing the “lysogenic” phenotype	This study
CSK47	<i>S. aureus</i>	CSK45 <i>geh</i> ::pCSK9 expressing the “lytic” phenotype	This study
CSK48	<i>S. aureus</i>	CSK45 <i>geh</i> ::pCSK9 expressing the “lysogenic” phenotype	This study
CSK56	<i>S. aureus</i>	CSK46 <i>geh</i> ::pCL25	This study
CSK59	<i>S. aureus</i>	8325-4/pNZlac	This study
CSK68	<i>S. aureus</i>	CSK45 <i>geh</i> ::pCL25	This study

Table 2. Plasmids used in this study. Plasmid name, a short description, and reference included for all plasmids.

Plasmid	Description	Reference or source
pDG1729	Promoterless LacZ reporter plasmid integrating in <i>B. subtilis</i> in <i>thrC</i>	(Guérout-Fleury, Frandsen and Stragier, 1996)
pNZlac	Promoterless replicative LacZ reporter plasmid	(Kovács <i>et al.</i> , 2010)
pCSK2	ϕ 13 switch inserted in pDG1729, <i>lacZ</i> fused to P _L downstream of <i>mor</i>	This study
pCSK3	ϕ 13 switch inserted in pNZlac, <i>lacZ</i> fused to P _L downstream of <i>mor</i>	This study
pCL25	Promoterless integration plasmid integrating into <i>attB</i> ^{L54a} in <i>geh</i> of <i>S. aureus</i>	(Luong and Lee, 2007)
pYL112 Δ 19	Contains L54a integrase. Needed for integration of pCL25 derivatives in <i>S. aureus</i>	(Lee, Buranen and Zhi-Hai, 1991)
pCSK9	ϕ 13 switch and <i>lacZ</i> of pCSK2 inserted in pCL25	This study
pCSK11	As pCSK2, with disrupted <i>mor</i> start codon (ATG to ATC)	This study
pCSK12	As pCSK9, with disrupted <i>mor</i> start codon (ATG to ATC)	This study
pCSK13	As pCSK3, with disrupted <i>mor</i> start codon (ATG to ATC)	This study
pET30a(+)	Expression vector containing ϕ 13 rCI gene	This study

Table 3. Phages used in this study. Phages used, a brief description of these, and a reference of origin included.

Phage	Description	Reference
φ13-kana	Fully functional φ13 containing a kanamycin resistance cassette	(Tang <i>et al.</i> , 2017)
φ11	Generally transducing <i>S. aureus</i> phage	(Novick, 1967)
φ80α	Generally transducing <i>S. aureus</i> phage	(Novick, 1963)
SPP1	Generally transducing <i>B. subtilis</i> phage	(Riva, Polsinelli and Falaschi, 1968)

Table 4. Frequencies of colonies with “lysogenic” phenotype after the introduction of φ13 switch plasmids into *S. aureus* or *B. subtilis* by transformation. Switch plasmids were replicative (pCSK3) or required integration into the host (pCSK9 in *S. aureus*, pCSK2 in *B. subtilis*). Recipient bacteria were naïve (*S. aureus* 8325-4 or *B. subtilis* 168) or φ13 lysogens (*S. aureus* 8325-4 φ13-kana). The number of biological replicates with more than 100 resulting colonies is stated in brackets. Frequencies of “lysogenic” transformant colonies on plates containing X-gal were calculated as the frequency between “lytic” and “lysogenic” in each transformation event and the average is shown here. Standard deviations are based on differences between each event.

<i>S. aureus</i> 8325-4		<i>S. aureus</i> 8325-4 φ13-kana		<i>B. subtilis</i> 168	
pCSK3*	pCSK9†	pCSK3**	pCSK9†	pCSK3	pCSK2
4.9 % ± 2.9 % (n=6)	12 % ± 10 % (77 colonies in total, n=5)	99.6 % ± 0.5 % (n=4)	100 % ± 0 % (63 colonies in total, n=9)	3.8 % ± 1.6 % (n=10)	3.0 % ± 1.6 % (n=18)

† indicates less than 100 transformants obtained in each experiment. The number of “lytic” and “lysogenic” colonies obtained in total for all replicas followed by the total count of biological replicates (n) for each event are stated in brackets. *) Re-transformation of 8325-4 by pCSK3 plasmids extracted from “lytic” and “lysogenic” colonies of 8325-4/pCSK3 yielded frequencies of “lysogenic” transformant colonies of 11 % and 5 %, respectively. **) Re-transformation of 8325-4 by pCSK3 plasmids extracted from “lytic” and “lysogenic” colonies of 8325-4 φ13-kana/pCSK3 yielded frequencies of “lysogenic” transformant colonies of 3 % and 11 %, respectively. When these plasmids were used to transform 8325-4 φ13-kana, 100 % “lysogenic” transformants were obtained.

FIGURE LEGENDS

Figure 1. Comparison of switch regions from *S. aureus* phage ϕ 13, *L. lactis* phage TP901-1, and *E. coli* phage λ . The geometry of the switch region is not shown to scale. The *mor* gene of TP901-1 and ϕ 13 is shown as a red box, the *cro* gene of λ is shown as a purple box, and the first part of the *cl* gene encoding the DNA binding N-terminal domain (CI-NTD) is shown as a blue box. The part of the *cl* gene from ϕ 13 encoding the extreme C-terminal domain (CI-CTD₂) is not homologous to the CI-CTD₂ domain in TP901-1 but to the C-terminal domain from CI of λ , containing a peptidase domain. CI-CTD₂ is shown as a green box for TP901-1 and a yellow box for ϕ 13 and λ . A dimerization domain (CI-CTD₁) with helical hook structures in TP901-1 connects CI-CTD₂ and CI-NTD and is shown as a black box for TP901-1 and ϕ 13, while the dimerization region is shown as a grey box for λ . The divergently oriented promoters, P_R and P_L for TP901-1, P_{RM} and P_R for λ , and putative P_R and P_L promoters for ϕ 13, are shown as arrows preceded by small black boxes symbolizing -10 and -35 regions. Small white boxes indicate ribosomal binding sites. Operators O_R, O_L, and O_D, recognized by the CI-NTD in TP901-1, homologous regions for ϕ 13, and operators O_{R1}, O_{R2}, and O_{R3} for λ , are shown as blue arrows. Figure inspired by Pedersen *et al.*, 2020.

Figure 2. EMSA of rCI repressor binding to putative operators O_R, O_L, and O_D in the ϕ 13 switch. A) Nucleotide sequence of the DNA fragments carrying ϕ 13 O_L, O_R, and O_D. Operator sites are underlined in blue. B) Fluorescent scan of agarose gels from EMSA employing ϕ 13 rCI and DNA fragments carrying O_L, O_R, and O_D and of agarose gels from EMSA employing ϕ 13 rCI and DNA fragments carrying mutated operator sites, in which the central C in each half-operator site was exchanged for a G: O_R^{control}, O_L^{control}, and O_D^{control}. Lane numbers are listed, where the concentration of rCI in lane 1 is 16.9 μ M and in the following lanes diluted serially by 2-fold dilutions. Lane 20 contains free unbound DNA. Black arrows point at bands with unbound DNA probe and red arrows point at bands for CI-bound DNA probe. Smears at high CI concentrations are presumed to be CI complexes bound to DNA probe. C) Analysis of the degree of binding (CI-bound DNA/(unbound DNA + CI-bound DNA) from quantification of the bands for unbound DNA probe (black arrows in B) and the bands for CI-bound DNA probe (red arrows in B), using the non-linear curve fitting option using the specific binding with Hill slope option in Graph Prism. Binding curves, dissociation constants, and Hill coefficients from the best fits are shown. Triplicate biological replicas were analyzed for the

1
2
3
4 determination of specific binding and standard deviations from these are shown. D) Analysis of the
5 degree of binding (calculated as (DNA in lane 20 – free DNA)/ DNA in lane 20) from quantification
6 of only the bands for unbound DNA probe (black arrows in B). Binding curves, dissociation constants,
7 and Hill coefficients from the best fits are shown. Triplicate biological replica were analyzed for the
8 determination of specific binding, and error bars represent \pm one standard deviation.
9
10
11
12
13
14
15
16

17 **Figure 3. Reporter plasmids for monitoring switching of the ϕ 13 switch in *B. subtilis* and *S. aureus*.**

18 The genetic switch of ϕ 13 was inserted into the reporter plasmids pDG1729 (pCSK2), pNZlac
19 (pCSK3), and pCL25 (pCSK9), allowing expression of the *lacZ* reporter gene at P_L activity. pCSK3 is
20 capable of replication in *B. subtilis*, while pCSK2 lacks a replicon and needs to integrate by
21 homologous recombination into the *thrC* gene of *B. subtilis*. pCSK9 integrates into the *attB*^{L54a}
22 integration site in *S. aureus*, facilitated by a L54a integrase supplied by pYL112 Δ 19. Plasmid maps
23 are not to scale. Restriction sites used for insertion of the switch DNA are shown. *cl* and *mor* of the
24 ϕ 13 genetic switch are illustrated in a lighter grey. Other contained genes: *spc*: spectinomycin
25 resistance not expressed in *S. aureus*, *lacZ*^{*E. coli*}: beta-galactosidase gene originating from *E. coli* fused
26 to the ribosome binding site of *B. subtilis spoVG*, '*hom*, *thrC*', '*thrC*, and *thrB*': segments of the genes
27 flanking the integration site of pCSK2 in *B. subtilis* allowing integration by homologous
28 recombination, *LacZ*^{*B. coagulans*}: beta-galactosidase gene originating from *B. coagulans*, *repA* and *repC*:
29 replicon A and C, *Cm*: chloramphenicol resistance gene, *tet*: tetracycline resistance, *attP*^{L54a}: L54a
30 phage attachment region.
31
32
33
34
35
36
37
38
39
40
41
42
43
44

45 **Figure 4. ϕ 13-kana infection of *S. aureus* 8325-4 transformants carrying switch plasmids.** Bacterial
46 strains A) 8325-4 *geh*::pCL25 (CSK68), B) 8325-4/pNZlac (CSK59), C) "lysogenic" 8325-4 *geh*::pCSK9
47 (CSK48), D) "lytic" 8325-4 *geh*::pCSK9 (CSK47), E) "lysogenic" 8325-4/pCSK3 (CSK33), and F) "lytic"
48 8325-4/pCSK3 (CSK32) were infected by bacteriophage ϕ 13-kana at a MOI of 0.1. Phage production
49 was quantified by normalizing the number of phages (determined as PFU ml⁻¹ of the culture
50 supernatant two hours after infection) by the CFU ml⁻¹ of the bacterial culture before infection. A)
51 and B) are controls where the strains contain the empty vectors used for the construction of pCSK9
52
53
54
55
56
57
58
59
60

1
2
3
4
5
6
7
8
9
10
11
12
13
14
15
16
17
18
19
20
21
22
23
24
25
26
27
28
29
30
31
32
33
34
35
36
37
38
39
40
41
42
43
44
45
46
47
48
49
50
51
52
53
54
55
56
57
58
59
60

and pCSK3, respectively. Bars represent the mean value of three replicate experiments, while error bars represent standard deviations.

Figure 5. Induction of “lysogenic” transformants of *B. subtilis* 168 and *S. aureus* 8325-4 by mitomycin C, ciprofloxacin, and hydrogen peroxide. Bacteria from a “lysogenic” (white) colony of *S. aureus* 8325-4 *geh*::pCSK9 (CSK48, left) and *B. subtilis* 168 *thrC*::pCSK2 (CSK9, right) were suspended in media and plated on X-gal plates. After drying, a drop of mitomycin C (top), ciprofloxacin (middle), or hydrogen peroxide (bottom) was applied in the middle. The plate was incubated overnight at 37 °C. Estimated MIC (minimal inhibitory concentration) and MTC (minimal toggle-inducing concentration) values are shown as red and black arrows, respectively. The MTC value of *B. subtilis* 168 *thrC*::pCSK2 exposed to hydrogen peroxide cannot be determined, but an estimate is suggested by a dashed arrow.

Figure 6. Toggle switching of “lysogenic” cells in response to mitomycin C. Bacteria from a “lysogenic” (white) transformant of A) 8325-4 *geh*::pCSK9 (CSK48) and B) *B. subtilis* 168 *thrC*::pCSK2 (CSK9) were plated, and a small drop of mitomycin C was immediately placed in the center. After growth overnight, individual colonies at different distances to the mitomycin C application spots were picked and suspended in medium without mitomycin C, from which dilutions were plated on LB/TSA X-gal plates. The frequency of colonies with the “lytic” (blue) phenotype was determined and plotted against the distance to the mitomycin C application. Lines have been inserted to illustrate the relationship between colonies on the plates and the determined frequencies of toggle switching.

Figure 7. Induction of “lysogenic” to “lytic” toggle switching from pCSK9 plasmids in *S. aureus* by temporal exposure to mitomycin C. “Lysogenic” 8325-4 *geh*::pCSK9 (CSK48) cells were grown in liquid TSB medium (in duplicates) and induced by addition of 1 $\mu\text{g ml}^{-1}$ mitomycin C at time=0 min. At the indicated times, aliquots were harvested and dilutions were plated on TSA plates containing X-gal. The average fraction of colonies (in %) with the “lytic” phenotype was plotted against the duration (in min) of the exposure to mitomycin C.

APPENDIX

APPENDIX FIGURES

Appendix Figure 1. The protein sequence of ϕ 13 rCI used in this study. The added tag is marked with a black box and consists of the His-tag (HHHHHH) and a TEV cleavage site (ENLYFQG). Cleavage of the tag leaves the G.

Appendix Figure 2. Sequence alignments of CI from *L. lactis* phage TP901-1, *S. aureus* phage ϕ 13, and *E. coli* phage λ (top) and MOR from TP901-1 and ϕ 13 (bottom). Identical and similar residues are shown in grey. Known domains are indicated by lines and designated by brief descriptions. The overall similarity between the CI repressors from ϕ 13 and TP901-1 is 51 % identical residues, while the local domain similarity for the NTD and CTD₁ is 71 % and 39 %, respectively. The overall similarity between CI from ϕ 13 and λ is 19 % identical residues, where the N-terminal parts only show similarities in the DNA binding domains. In the C-terminal part, where λ carries its peptidase domain required for autocleavage, the local similarity is 21 %, but the catalytic Ser and Lys residues and the G-residue of the autocleavage site are conserved. The overall similarity for the MOR anti-repressors from ϕ 13 and TP901-1 is 65 %.

Appendix Figure 3. Purification and characterization of tagged ϕ 13 rCI. A) SEC chromatogram of ϕ 13 rCI. The absorbance at 260 and 280 nm are shown in red and blue, respectively. The largest peak eluted at 177.2 ml corresponding to a tetramer. B) SDS-PAGE gel showing the different steps of expression and purification of ϕ 13 rCI. Lane 1: Precision Plus Protein™ Dual Xtra Prestained Protein Standard marker, lane 2: cell pellet diluted in water, lane 3: cell lysate after sonication and centrifugation, lane 4: HisTrap HP 1 ml flowthrough, lane 5: HisTrap HP 1 ml eluate, lane 6-10: five fractions from SEC covering the peak from 110 to 185 ml. The molecular weights of standards in kDa are shown on the left. C) the first derivative of the ratio between 350 and 330 nm measured with DSF. The point of the inflection temperature is marked with a diamond. D) CD spectrum of ϕ 13 rCI with the results from the deconvolution using BeStSel and DichroWeb inserted as pie charts. The

predicted secondary structure types of helix, strand, turns, and unordered are colored blue, yellow, red, and green, respectively, for both BeStSel and DichroWeb predictions.

APPENDIX TABLES

Appendix Table 1. A complete list of bacterial strains used in this study. Strain, species, a short description, and reference of all strains used in this study. See main text for a reference list.

Strain	Species	Short description or relevant genotype	Reference or source
168	<i>B. subtilis</i>		(Burkholder and Giles, 1947)
8325-4	<i>S. aureus</i>	NCTC8325 phage cured	(Novick, 1967)
8325-4 ϕ 13-kana	<i>S. aureus</i>	8325-4 lysogenized with ϕ 13-kana	(Tang <i>et al.</i> , 2017)
IM08B	<i>E. coli</i>	K12 DH10B Δdcm <i>hsdMS</i>	(Monk <i>et al.</i> , 2015)
CSK8	<i>B. subtilis</i>	168 <i>thrC</i> ::pCSK2 expressing the "lytic" phenotype	This study
CSK9	<i>B. subtilis</i>	168 <i>thrC</i> ::pCSK2 expressing the "lysogenic" phenotype	This study
CSK10	<i>B. subtilis</i>	168/pCSK3 expressing the "lytic" phenotype	This study
CSK11	<i>B. subtilis</i>	168/pCSK3 expressing the "lysogenic" phenotype	This study
CSK19	<i>E. coli</i>	IM08B/pCSK3	This study
CSK26	<i>E. coli</i>	IM08B/pCSK9	This study
CSK32	<i>S. aureus</i>	8325-4/pCSK3 expressing the "lytic" phenotype	This study
CSK33	<i>S. aureus</i>	8325-4/pCSK3 expressing the "lysogenic" phenotype	This study
CSK44	<i>E. coli</i>	IM08B/pYL112 Δ 19	This study
CSK45	<i>S. aureus</i>	8325-4/pYL112 Δ 19	This study
CSK46	<i>S. aureus</i>	8325-4 ϕ 13-kana/pYL112 Δ 19	This study
CSK47	<i>S. aureus</i>	CSK45 <i>geh</i> ::pCSK9 expressing the "lytic" phenotype	This study

CSK48	<i>S. aureus</i>	CSK45 <i>geh</i> ::pCSK9 expressing the “lysogenic” phenotype	This study
CSK50	<i>S. aureus</i>	8325-4 ϕ 13-kana/pCSK3 expressing the “lysogenic” phenotype	This study
CSK51	<i>S. aureus</i>	8325-4 ϕ 13-kana/pCSK3 expressing the “lytic” phenotype	This study
CSK52	<i>S. aureus</i>	8325-4 ϕ 13-kana <i>geh</i> ::pCSK9 expressing the “lysogenic” phenotype	This study
CSK54	<i>E. coli</i>	IM08B/pCL25	This study
CSK56	<i>S. aureus</i>	CSK46 <i>geh</i> ::pCL25	This study
CSK57	<i>E. coli</i>	IM08B/pNZlac	This study
CSK59	<i>S. aureus</i>	8325-4/pNZlac	This study
CSK60	<i>S. aureus</i>	8325-4 ϕ 13-kana/pNZlac	This study
CSK65	<i>E. coli</i>	IM08B/pCSK12	This study
CSK67	<i>S. aureus</i>	CSK46 <i>geh</i> ::pCSK12 expressing the “lysogenic” phenotype	This study
CSK68	<i>S. aureus</i>	CSK45 <i>geh</i> ::pCL25	This study
CSK69	<i>S. aureus</i>	CSK45 <i>geh</i> ::pCSK12 expressing the “lysogenic” phenotype	This study
CSK70	<i>B. subtilis</i>	168 <i>thrC</i> ::pCSK11 expressing the “lysogenic” phenotype	This study
CSK77	<i>E. coli</i>	IM08B/pCSK13 expressing the “lysogenic” phenotype	This study
CSK78	<i>S. aureus</i>	8325-4/pCSK13 expressing the “lysogenic” phenotype	This study
CSK79	<i>S. aureus</i>	8325-4 ϕ 13-kana/pCSK13 expressing the “lysogenic” phenotype	This study
CSK80	<i>B. subtilis</i>	168/pCSK13 expressing the “lysogenic” phenotype	This study

Appendix Table 2. Primers used in this study. Name and sequence of primers used for plasmid construction and gel shift assays. All were primers designed specifically for this study.

Primer name	Sequence (5' to 3')
MK740	Cy5-GTAATACGACTCACTATAGG
MK741	Cy5-CCTTTTGTGTGAAAGTTACC
MK860	AAAAGGATCCGTGATTTGTTCCATTGTGC
MK861	AAATCTAGATTAAAGCGCTAAATATACGTTATTAATCAC
MK862	AAAAGCATGCGTGATTTGTTCCATTGTGC
MK863	AAAAGAATTCTTAAAGCGCTAAATATACGTTATTAATCAC
MK867	GTAATACGACTCACTATAGGATAATAAAGCTTGTGAACAAAATTC
MK868	CCTTTTGTGTGAAAGTTACCACTTTACACCTGTTTTGAATC
MK869	GTAATACGACTCACTATAGGGACTTGATTCAAAACAAGGTGTAAG
MK870	CCTTTTGTGTGAAAGTTACCTGAGTAGTCGTAACACATAAAAAGC

MK871	GTAATACGACTCACTATAGGATATACCGGTAGAGAAAATACAC
MK872	CCTTTTGTGTGAAAAGTTACCGGATCCGTGATTTGTTCCATTGTG
MK902	AAAAAGATCTGCAGACATGGCCTGCC
MK1038	GTTGAACAAAAATTCAACAAAAAGTTGATAAATCATCAATTTTTGTATTG
MK1039	CAATACAAAAATTGATGATTTATCAACTTTTTGTTGAATTTTTGTTCAAC
MK1040	CAAAACAAGGTGTAAAGTATAGTTAAGTTGATGATACGTCAACTTGAGAGGAG
MK1041	CTCCTCTCAAGTTGACGTATCATCAACTTAACTATACTTTACACCTTGTTTTG
MK1042	CACTTATATTTTTTAAAGAAAAAGTTGATGTTATATCAACTTAAGGAGGGGCAC
MK1043	GTGCCCTCCTTAAGTTGATATAACATCAACTTTTTCTTTAAAAAAATATAAGTG

Appendix Table 3. Lysogenization frequency after ϕ 13-kana infection of *S. aureus* 8325-4 and comparison to transformation of 8325-4 by pCKS3. *S. aureus* strain 8325-4 was infected with ϕ 13-kana at multiplicity of infection (MOI) at 1 and 0.1, and the frequency of lytic events (phage titer in PFU/ml, column 1) as well as the frequency of lysogenic events (CFU/ml after plating infected cells on TSB plates containing kanamycin, column 2). Column 3 shows the lysogenization frequency for all bacteria infected by ϕ 13-kana (lysogenic events / (lytic events + lysogenic events)) for 5 biological replicates. Column 4 shows the MOI. Five biological replicates were included for both MOI 1 and MOI 0.1. Average lysogenization frequencies are shown in column 5. The P-values from two-sample *t*-tests of average frequency from the infections at MOI of 1 and 0.1 against the frequency observed at transformation of 8325-4 by pCKS3 (4.9 % \pm 2.9 %) are shown in column 6.

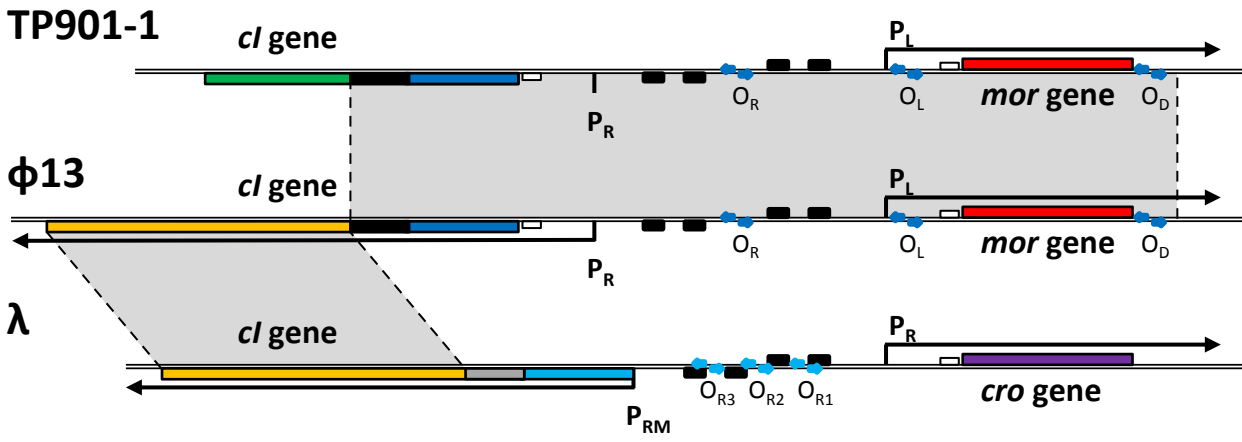
lytic events (PFU ml ⁻¹)	lysogenic events (CFU(Kan ^R)ml ⁻¹)	Lysogenization frequency (%)	MOI	Average lysogenization frequency	(P-value for mean equal to pCKS3)
2.8E+07	2.9E+06	9.4	1	4.6 % \pm 2.8 %	0.87
1.1E+08	2.9E+06	2.6	1		
7.2E+06	3.2E+05	4.3	1		
1.5E+07	7.2E+05	4.6	1		
2.5E+07	6.2E+05	2.4	1		
1.9E+06	1.9E+05	9.1	0.1	3.5 % \pm 3.3 %	0.47
1.2E+07	3.8E+05	3.1	0.1		
8.5E+05	2.1E+04	2.4	0.1		
5.5E+07	4.9E+04	0.1	0.1		
1.1E+07	3.2E+05	2.8	0.1		

Appendix Table 4. Frequencies of colonies with the “lysogenic” phenotype after the introduction of *mor*-deficient ϕ 13 switch plasmids into *S. aureus* or *B. subtilis* by transformation. Switch plasmids were replicative (pCSK13) or required integration into the host (pCSK12 in *S. aureus*, pCSK11 in *B. subtilis*). pCSK11-13 are *mor*-deficient versions of pCSK2, pCSK9, and pCSK3, respectively. Recipient bacteria were naïve (*S. aureus* 8325-4 or *B. subtilis* 168) or ϕ 13 lysogens (*S. aureus* 8325-4 ϕ 13-kana). The number of biological replicates with more than 100 resulting colonies are stated in brackets. Frequencies of “lysogenic” transformant colonies on plates containing X-gal were calculated as the frequency between “lytic” and “lysogenic” in each transformation event and the average is shown here. Standard deviations are based on differences between each event.

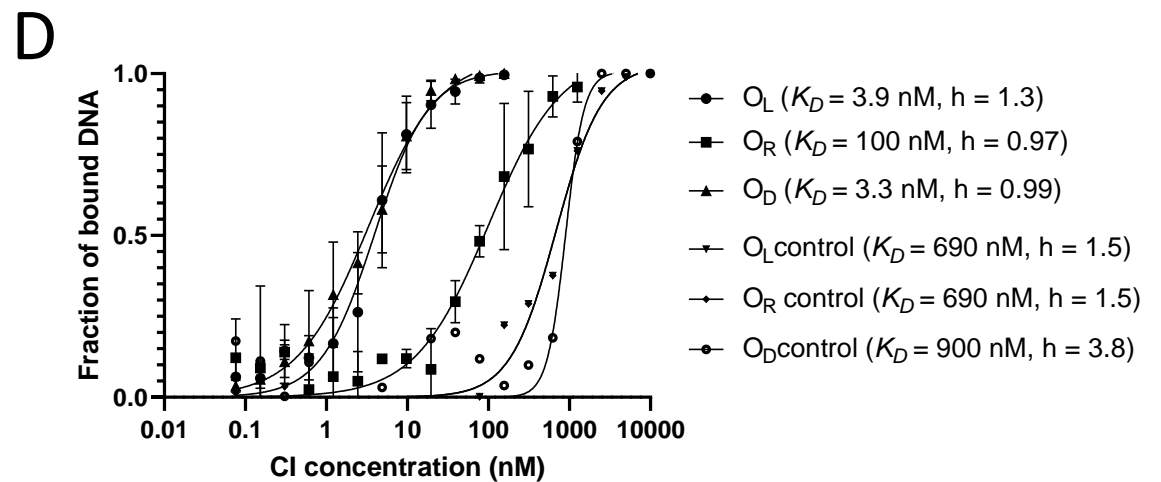
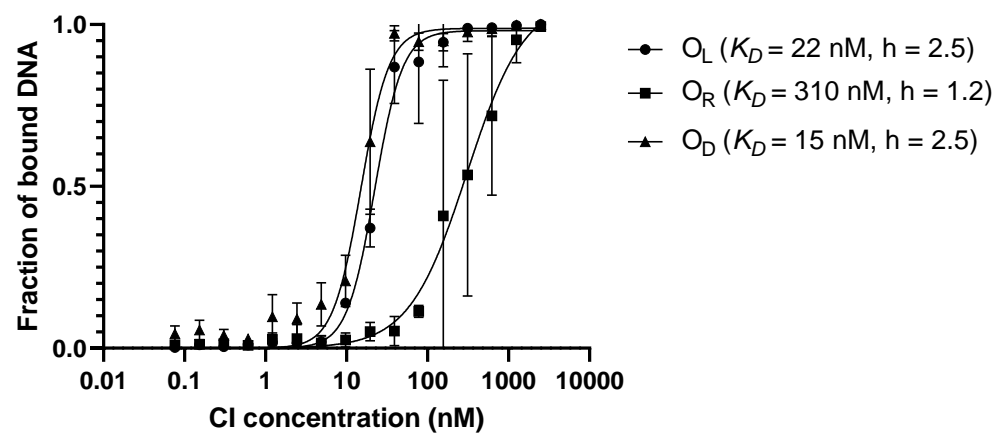
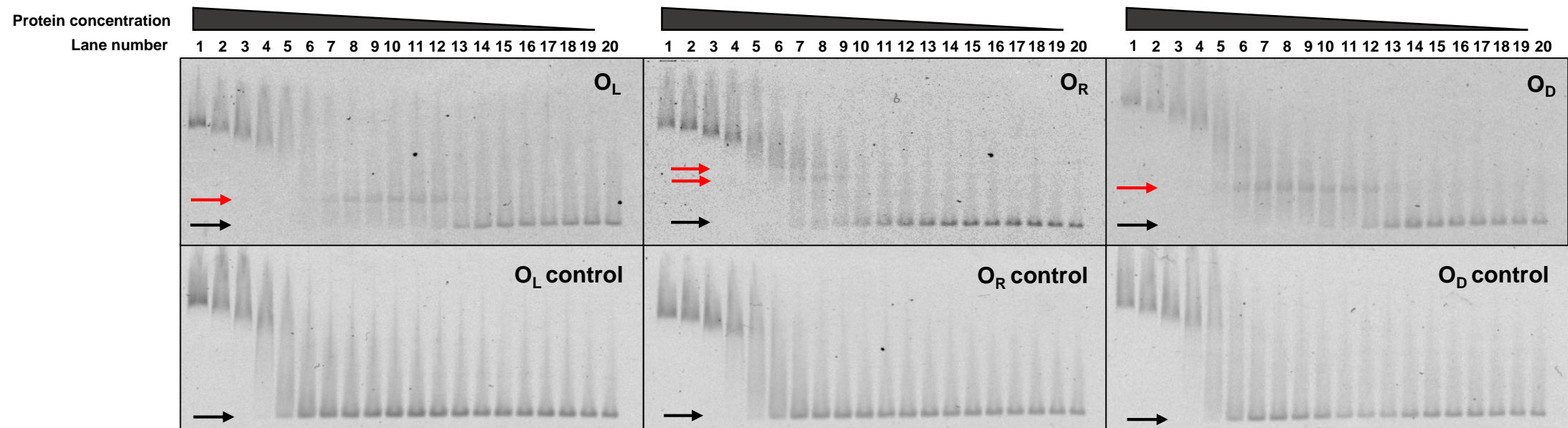
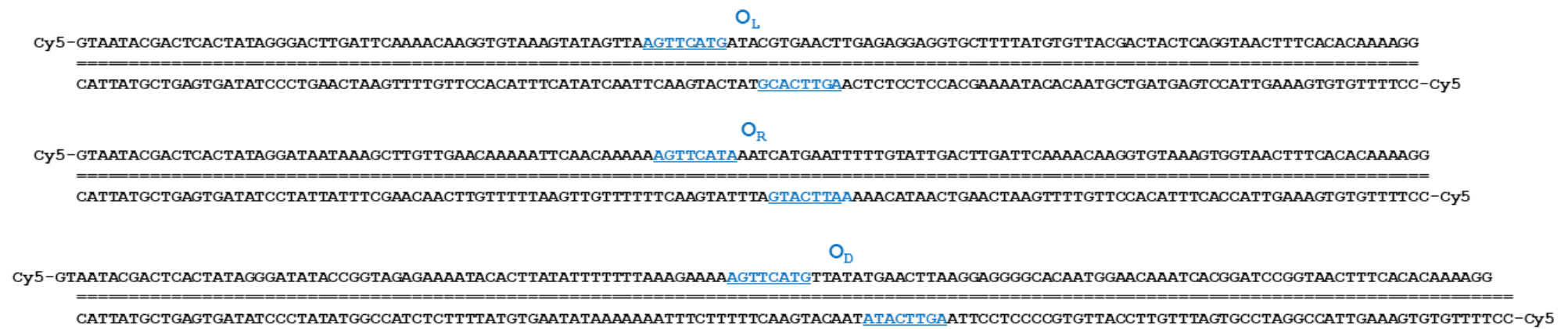
<i>S. aureus</i> 8325-4		<i>S. aureus</i> 8325-4 ϕ 13-kana		<i>B. subtilis</i> 168	
pCSK12 [†]	pCSK13 [†]	pCSK12 [†]	pCSK13	pCSK11	pCSK13
100.0 ± 0 (99 colonies in total; n=3)	100.0 ± 0 (440 colonies in total; n=6)	100.0 ± 0 (477 colonies in total; n=4)	100.0 ± 0 (n=6)	100.0 ± 0 (n=3)	100.0 ± 0 (n=4)

[†] indicates that less than 100 transformants obtained in some or all experiments. The total number of colonies is stated in brackets.

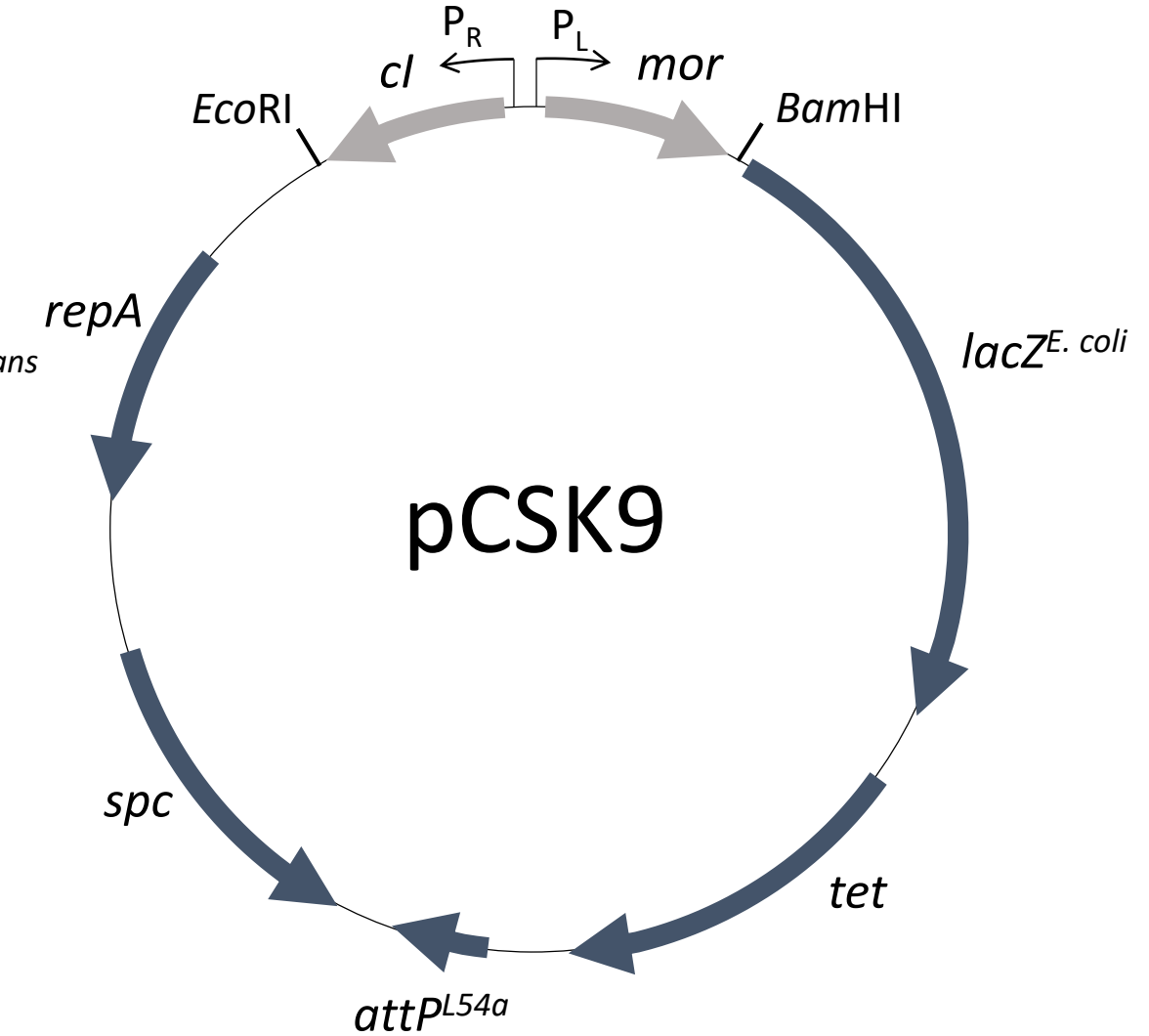
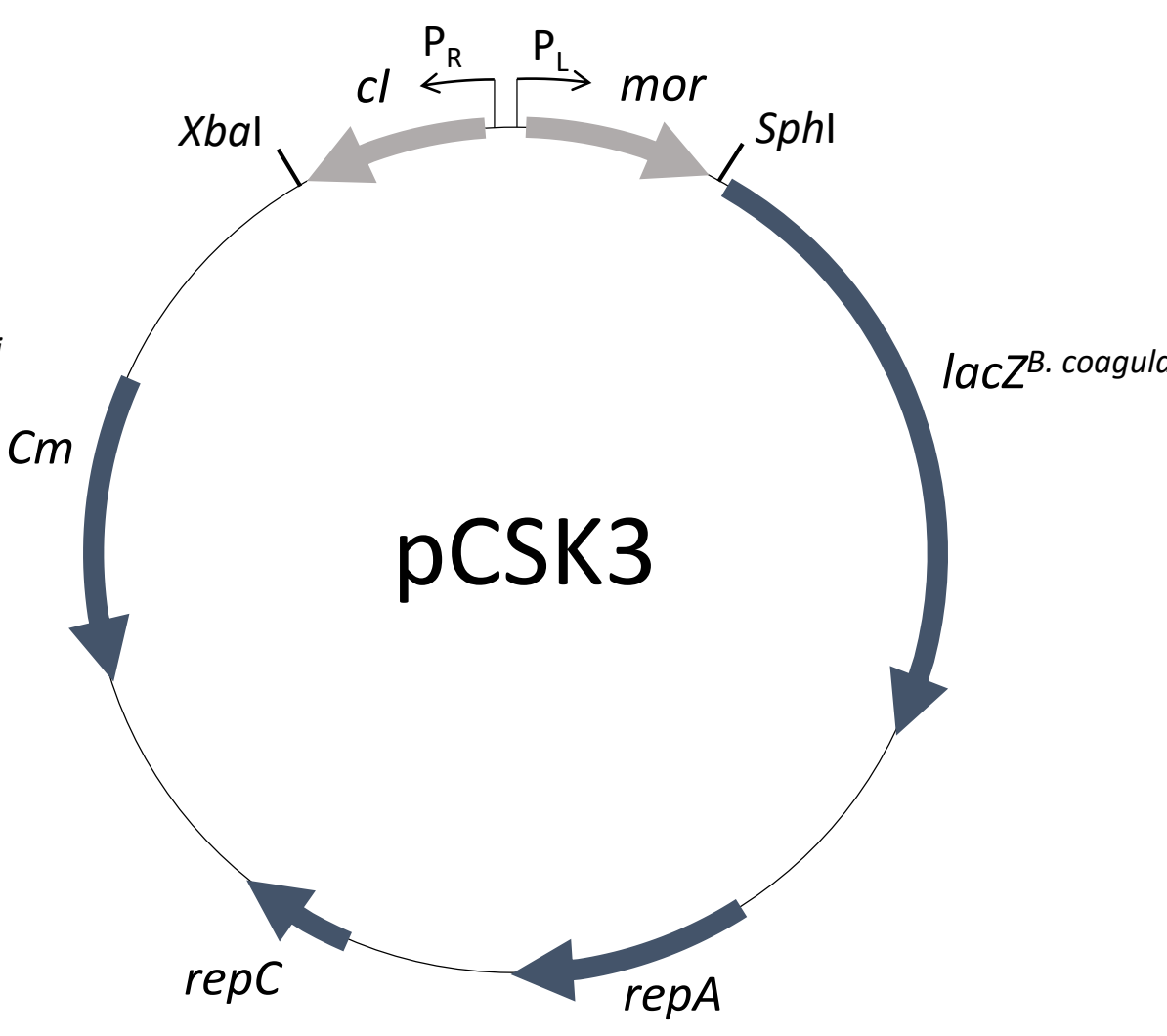
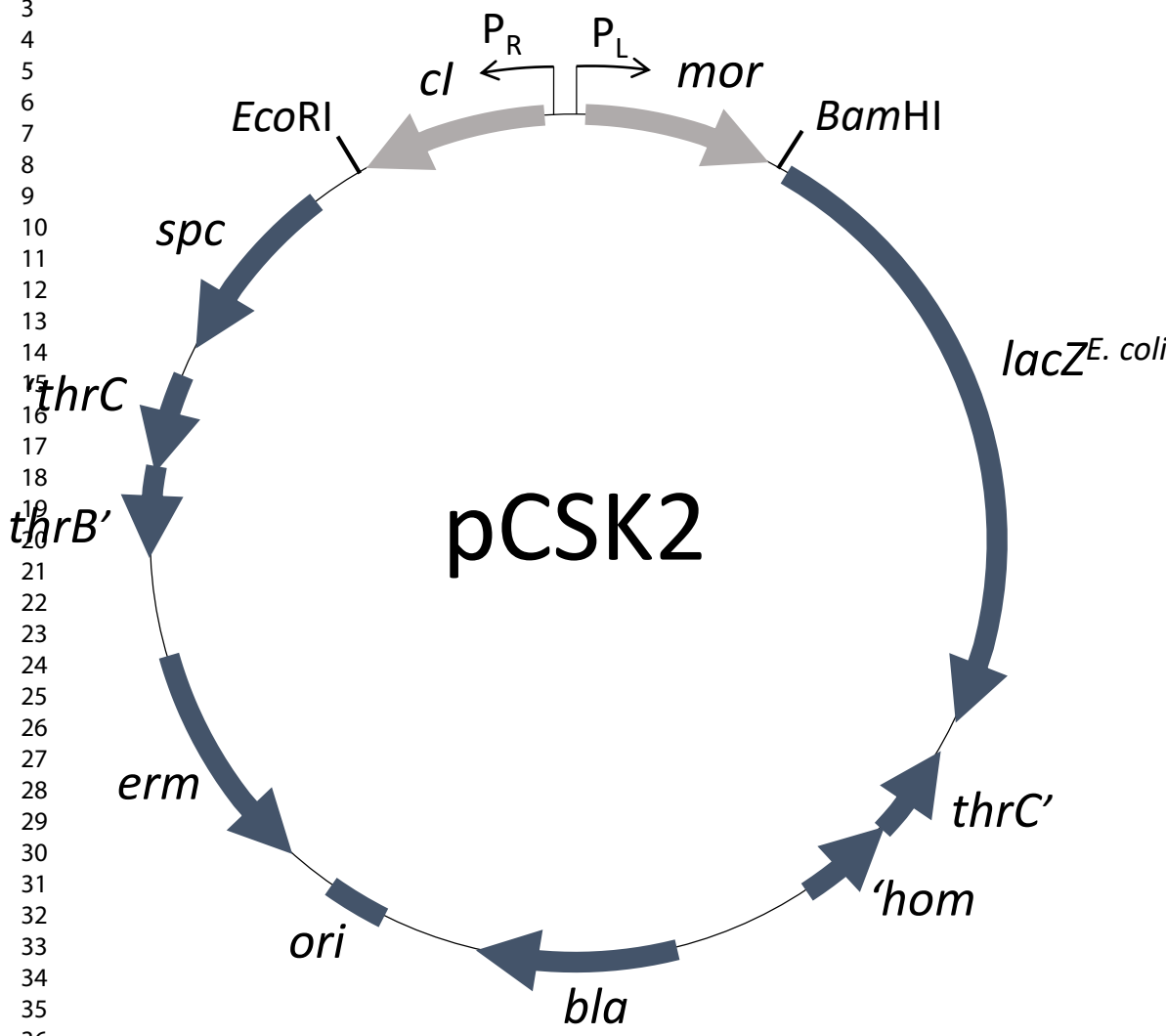
1
2
3
4
5
6
7
8
9
10
11
12
13
14
15
16
17
18
19
20
21
22
23
24
25
26
27
28
29
30
31
32
33
34
35
36
37
38
39
40
41
42
43
44
45
46
47
48
49
50
51
52
53
54
55
56

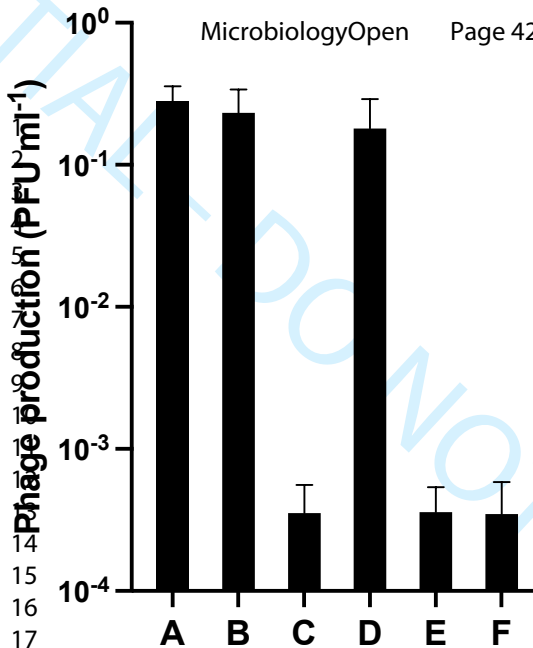


1
2
3
4
5
6
7
8
9
10
11
12
13
14
15
16
17
18
19
20
21
22
23
24
25
26
27
28
29
30
31
32
33
34
35
36
37
38
39
40
41
42
43
44
45
46
47
48
49
50
51
52
53
54
55
56
57
58
59
60

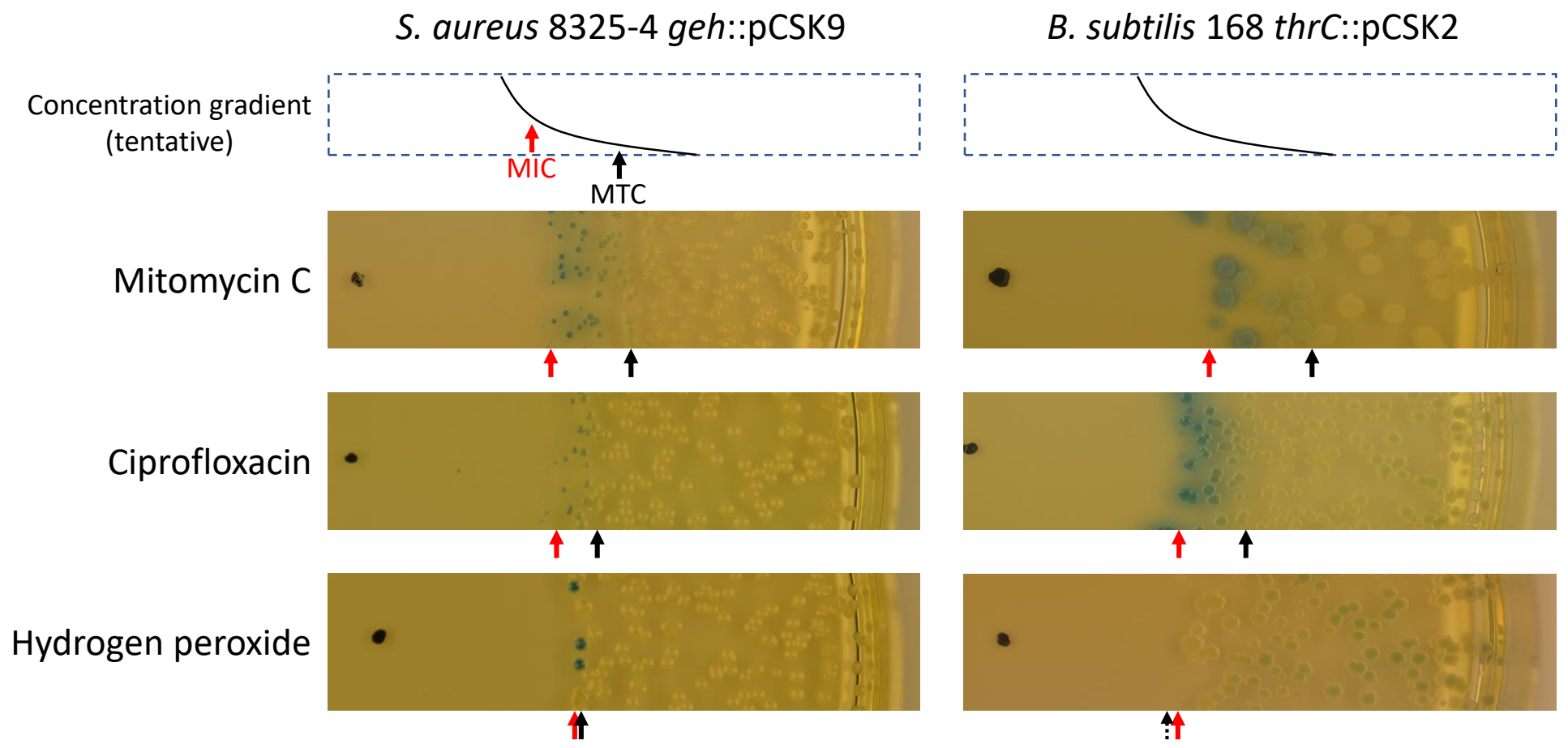


1
2
3
4
5
6
7
8
9
10
11
12
13
14
15
16
17
18
19
20
21
22
23
24
25
26
27
28
29
30
31
32
33
34
35
36
37
38
39
40
41

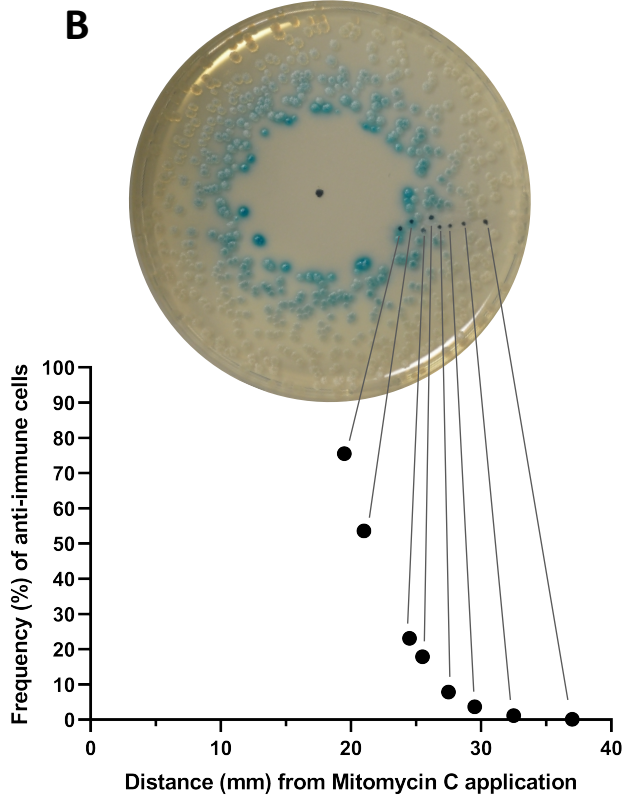
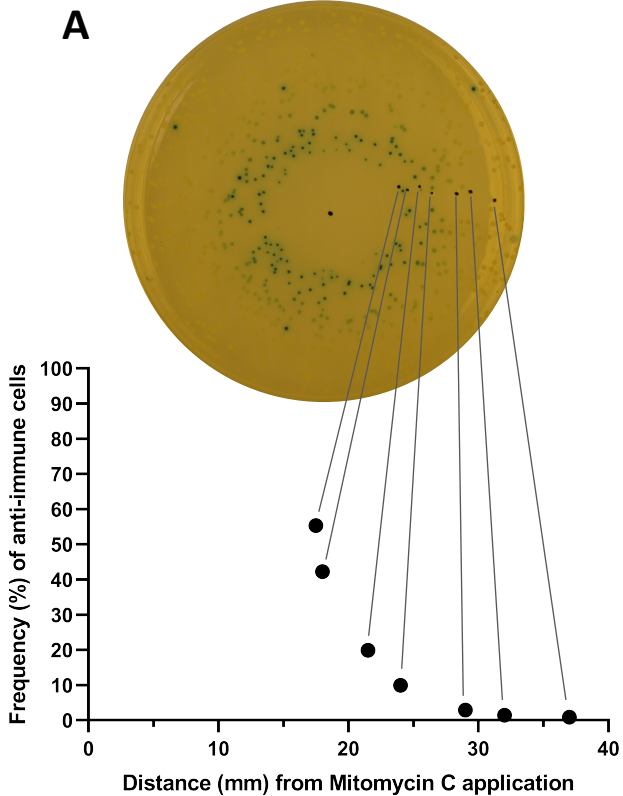


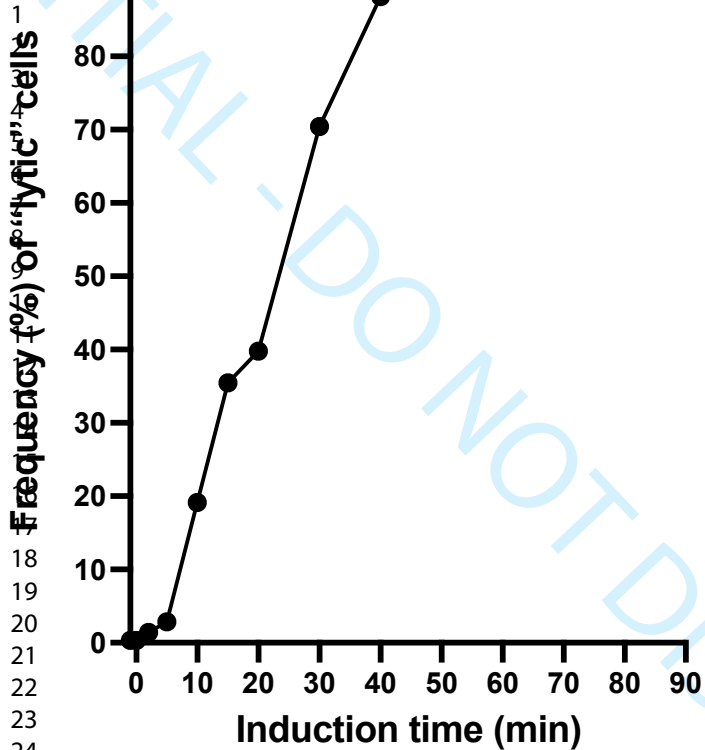


1
2
3
4
5
6
7
8
9
10
11
12
13
14
15
16
17
18
19
20
21
22
23
24
25
26
27
28
29
30
31
32
33
34
35
36
37
38
39
40
41



1
2
3
4
5
6
7
8
9
10
11
12
13
14
15
16
17
18
19
20
21
22
23
24
25
26
27
28
29
30
31
32
33
34
35
36
37
38
39
40
41





APPENDIX FIGURES

1
2
3
4
5
6
7
8
9
10 Phi13_CI-tagged 1 MKHHHHHPMSDYDIPPTENLYFOGMREKVSNRLKHIMKIRNLKQVDIINKSKPYQKKLG
11
12 Phi13_CI-tagged 61 ISLSKSTLSQYINDVQSPDQDRIYLLSKTLNVGEAWLMGYDVDSYRVPDEERQDETIMSK
13
14 Phi13_CI-tagged 121 INNIFSQLTTPRQENVLNYANEQLEEQNKVTSIDGYKESKLVSYIACGATGAGIGEELYD
15
16 Phi13_CI-tagged 181 DILHEEVFFKEDETSPNADFCILVNGDSMEPMLKQGTAFYAFIKKEDSIKDGTTIALVVLGCV
17
18 Phi13_CI-tagged 241 SLIKRVDICEDYINLVSLNPKYDDIKVASFSDIKVMGKVVV
19

Appendix Figure 1

CONFIDENTIAL - DO NOT DISTRIBUTE

20
21
22
23
24
25
26
27
28
29
30
31
32
33
34
35
36
37
38
39
40
41
42
43
44
45
46
47
48
49
50
51
52
53
54
55
56
57
58
59
60

CI**NTD (DNA binding and MOR interaction)**

6	Tp901-1	<u>MKTDTSNRLKQIMAERNLKQVDILNLSIPFQKKFGIKLSKSTLSQYVNSVQSPDQNR IYL</u>	60
7		M+ SNRLK IM RNLKQVDI+N S P+QKK GI LSKSTLSQY+N VQSPDQ+RIYL	
8	Φ13	<u>MREKVSNRLKHIMKIRNLKQVDIINKSKPYQKLGISLSKSTLSQYINDVQSPDQDR IYL</u>	60
9		L Q + K+G+ +S + N + + + L	
9	Lambda	31- <u>LSQESV-----ADKMGMG--QSGVGALFNGINALNAYNAAL</u>	66
		DNA binding (HTH)	

CTD1 (dimer interface)

12	Tp901-1	<u>LAKTLGVSEAWLMGFVPMVESSKIENDSENIEETI-----TVMKKLEEPQKVVLDTA K</u>	115
13		L+KTL V EAWLMG+D V+S ++ D E +ETI + +L PRQ+ VL+ A	
14	Φ13	<u>LSKTLNVGEAWLMGYD---VDSYRVP-DEERQDETIMSKINNIFSQ LTPPRQENVLN YAN</u>	116
15		L+K L V P R+ I+	
15	Lambda	<u>LAKILKVSVEEFS-----P-SIARE-----IY-----</u>	91

18	Tp901-1	<u>IQLKEQDEQNKVKQIEDYRLSDEYLEEQISKASAYGGGQLND---NDKEFFKRLLN TLK</u>	172
19		QL +EQNKV I+ Y+ S A G +L D +++ FFK	
20	Φ13	<u>EQL---EEQNKVTSIDGYKESKLVSYIACGATGAGIGEELYDDILHEEVFFKEDETP SNA</u>	173
21		+ S+ E + S++ G E E + + S++	
21	Lambda	<u>-----VSMQPSLRSEYEYPVFSHVQAGMF---SPELRTFTKGD AERWVSTTKKASDS</u>	139
		auto cleavage site (between A and G)	

24	Tp901-1	<u>EKIDKGD L*</u>	180
26	Φ13	<u>DFCILVNGDSME-----PMLKQGT YAFIKKEDSIKDG TIALVVL DGVSL- IKRVDICED</u>	226
27		F + V G+SM P G + E +++ G + L G K++	
27	Lambda	<u>AFWLEVEGNSMTAPTGSKPSFPDGMLLILVDPEQAVEPGDFCIARLGGDEFTFKKLIRDSG</u>	200
		catalytic Ser dimer interface catalytic Lys	

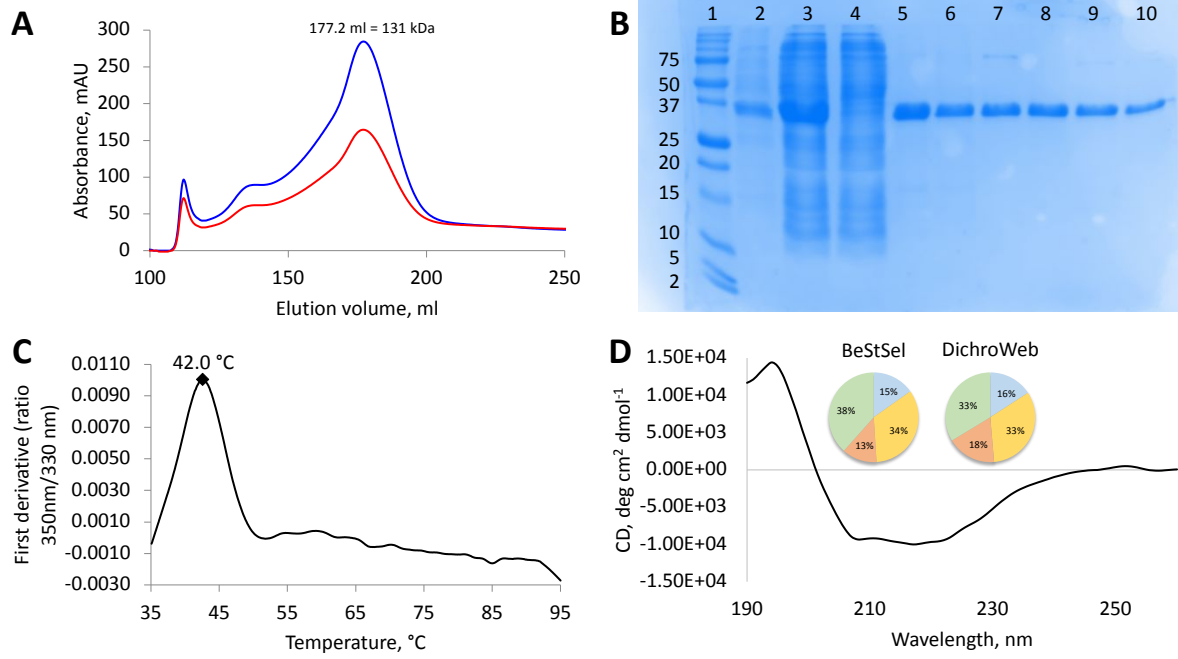
31	Φ13	<u>YINLVSLNPKYDDIKVASFS DIKVMGKVVL*</u>	256
32		+ L LNP+Y I V+GKV+	
33	Lambda	<u>QVFLQPLNPQYEMIPCN-ESCSVVGKVIASOWPEEIFG*</u>	237
		dimer interface	

MOR

38	Tp901-1	<u>MSYDYSSLLGKITEKCGTQYNFAIAMGLSERIVSLKLN DKVIWKDDEILKAVHVLELN PQ</u>	60
39		M YDYS L GKI EK GTQYNFAIAM LSER++SLKLN KV WKD EI KA+ +L++ +	
40	Φ13	<u>MCYDYSRLSGKIVEKYGTQYNFAIAMKLSERSLSLKLNGKVGWKDSEIWKAIQLLDIPVE</u>	60
42	Tp901-1	<u>DIPKYFFNAKVH</u>	72
43		I YFF KVH	
44	Φ13	<u>KIHLYFFKEKVH</u>	72

Appendix Figure 2.

I R I B U T E



Appendix Figure 3.

DO NOT DISTRIBUTE

1
2
3
4
5
6
7
8
9
10
11
12
13
14
15
16
17
18
19
20
21
22
23
24
25
26
27
28
29
30
31
32
33
34
35
36
37
38
39
40
41

